SINTER HARDENING STUDIES OF ASTALOY 85 MO POWDER WITH VARYING COPPER CONTENTS

A THESIS SUBMITTED TO
THE GRADUATE SCHOOL OF NATURAL AND APPLIED SCIENCES
OF
MIDDLE EAST TECHNICAL UNIVERSITY

BY

MEHMET DİNCER

IN PARTIAL FULFILLMENT OF THE REQUIREMENTS
FOR
THE DEGREE OF MASTER OF SCIENCE
IN
METALLURGICAL AND MATERIALS ENGINEERING

DECEMBER 2014

Approval of the thesis:

SINTER HARDENING STUDIES OF ASTALOY 85 MO POWDER WITH VARYING COPPER CONTENTS

submitted by **MEHMET DİNCER** in partial fulfillment of the requirements for the degree of **Master of Science in Metallurgical and Materials Engineering Department, Middle East Technical University** by,

Prof. Dr. Gülbin Dural Ünver _____
Dean, Graduate School of **Natural and Applied Sciences**

Prof. Dr. Hakan C. Gür _____
Head of Department, **Metallurgical and Materials Engineering**

Prof. Dr. Bilgehan Ögel _____
Supervisor, **Metallurgical and Materials Eng. Dept., METU**

Prof. Dr. Nuri Durlu _____
Co-Supervisor, **Mechanical Engineering Dept., TOBB ETU**

Examining Committee Members:

Prof. Dr. Rıza Gürbüz _____
Metallurgical and Materials Engineering Dept., METU

Prof. Dr. Bilgehan Ögel _____
Metallurgical and Materials Engineering Dept., METU

Prof. Dr. Nuri Durlu _____
Mechanical Engineering Dept., TOBB ETU

Assoc. Prof. Dr. Y. Eren Kalay _____
Metallurgical and Materials Engineering Dept., METU

Assist. Prof. Dr. Bilge İmer _____
Metallurgical and Materials Engineering Dept., METU

Date: 02.12.2014

I hereby declare that all information in this document has been obtained and presented with academic rules and ethical conduct. I also declare that, as required by those rules and conduct, I have fully cited and referenced all material and results that are not original to this work.

Name, Last Name: Mehmet Dincer

Signature:

ABSTRACT

SINTER HARDENING STUDIES OF ASTALOY 85 MO POWDER WITH VARYING COPPER CONTENTS

Dincer, Mehmet

M.S., Department of Metallurgical and Materials Engineering

Supervisor: Prof. Dr. Bilgehan Ögel

Co-supervisor: Prof. Dr. Nuri Durlu

December 2014, 92 Pages

In this thesis study, the effect of sinter hardening on mechanical properties of Astaloy 85 Mo (Fe - 0.85% Mo) powder with addition of 0.8% C and varying copper contents (1% Cu, 2% Cu) was examined. Powder mixes were compacted under 600 MPa. After compaction, the samples were sintered at 1120^{o}C under endogas from methane in an industrial sintering furnace and were sinter-hardened with three different cooling rates (0.5^{o}C/sec., 1.5^{o}C/sec., 3^{o}C/sec.). The study revealed that the cooling rate does not make critical changes on the microstructure of copper free samples. Addition of copper increased the hardenability of the samples which resulted formation of higher amount of martensite in the microstructure. The samples containing 2% Cu were nearly 100% martensitic. Also, the study showed that an increase in % Cu decreases the porosity content and increases the attained densities.

Keywords: powder metallurgy, Astaloy 85 Mo, sinter hardening

ÖZ

ÇEŞİTLİ BAKIR İÇERİĞİNE SAHİP ASTALOY 85 MO TOZLARININ SİNTERLEME İLE SERTLEŞTİRİLME ÇALIŞMALARI

Dincer, Mehmet

Yüksek Lisans, Metalurji ve Malzeme Mühendisliği

Tez Yöneticisi: Prof. Dr. Bilgehan Ögel

Ortak Tez Yöneticisi: Prof. Dr. Nuri Durlu

Aralık 2014, 92 sayfa

Bu tez çalışmasında, sinterleme ile sertleştirme işleminin 0.8% C ve değişen miktarlarda bakır (1% Cu, 2% Cu) içeren Astaloy 85 Mo (Fe – 0.85% Mo) tozlarının mekanik özelliklerine olan etkisi araştırılmıştır. Toz karışımları 600 MPa basınç altında preslenmiştir. Preslenen numuneler endüstriyel bir sinterleme fırınında 1120^{o}C'de ekzotermik gaz ortamında 20 dakika sinterlenmiştir. Sinterlemenin hemen ardından aynı fırında üç farklı soğutma hızı (0.5^{o}C/sn., 1.5^{o}C/sn., 3^{o}C/sn.) ile sinterleme ile sertleştirme işlemi yapılmıştır. Çalışma sonunda, soğutma hızının bakır içermeyen numunelerde ciddi bir etkisinin olmadığı gözlemlenmiştir. Bakırın eklenmesiyle sertleştirilebilirlik arttırılarak martensit miktarında belirgin bir artış gözlemlenmiştir. %2 bakır içeren numunelerde neredeyse tamamen martensitik yapı görülmüştür. Ek olarak, bakır oranındaki artış gözenek miktarında azalmaya dolayısıyla yoğunluk artışına olanak vermiştir.

Anahtar Kelimeler: Toz metalurjisi, Astaloy 85 Mo, sinterleme ile sertleştirme

To my precious family

ACKNOWLEDGMENTS

Firstly, I am grateful to Prof. Dr. Bilgehan Ögel for his great motivation, wise supervision, endless patience and never-ending belief in me and my study.

I would like to express my gratitude to Prof. Dr. Nuri Durlu for his valuable supervision, infinite patience and terrific support.

I would like to thank Hakan Hafızoğlu and Ahmet Murat Öge especially for their precious help during the experiments in TOBB ETU and Tozmetal A.Ş. company.

I would specially thank to Cengiz Tan and Serkan Yılmaz for their support and help about using of scanning electron microscope and Yusuf Yıldırım for his valuable recommandations and patient help about metallographic examinations.

I gratefully acknowledged to Tozmetal A.Ş. Company, general manager Hüsnü Özdural, design office and R&D manager Aytaç Ataş, and production and process control manager Cengiz Boyacı, for their support about the sintering and sinter-hardening of the samples.

I am grateful to my labmates, Gülten Kılıç and Güher Tan for their great friendship, brilliant guidance and splendid support during the difficult path of M.S. study. Special thanks Gülten and Güher for creating a warm workplace and building a indestructible family portrait from the beginning of my academical life.

I also thank to Evren Tan for his valuable support and outstanding motivation during this study.

Thanks to Onur Saka for always having joyful and great times together during all these years.

I also want to specially thank to my dearest friends and colleagues Bengi Yağmurlu and Kıvanç Korkmaz for their great motivation, unlimited support and valuable friendship.

I am grateful to Kerem Dönmez, Melike Nur Bostancı, Ayda Çiğlez, Umut İnce and Melis Çekicioğlu for their eternal confidence in my success and their immortal friendship.

Special thanks to Orkun Mugan and Utku Olgun who wish the best and help for the better throughout this journey.

Finally, I must also thank to my family, Nevin and Ünal, for everlasting patience and special faith about my success during my study. Their motivation and confidence to me always convinced me when I really wanted to quit during this long path. Nevin and Ünal is the real owner of this M.S. degree.

TABLE OF CONTENTS

LIST OF FIGURES

FIGURES

LIST OF TABLES

TABLES

CHAPTER 1

INTRODUCTION

Metallurgy basically deals with production of metal parts as final product for the use of human-being. There are different metal production techniques for different aims. Powder metallurgy is a branch of metal part production techniques that generally provides complex shape production. Importance and usage of powder metallurgy in industry increase day by day because of the advantages of this production technique. Nowadays, powder metallurgy is used for different applications areas and has a wide range of application from defense industry to houseware applications [1].

Powder metallurgy generally deals with metallic materials but other materials including polymeric materials, composite materials and ceramic materials, [1] can be manufactured by powder metallurgy. General production route for powder metallurgy consists of five fundamental steps. First stage is the manufacturing of the powders from bulk materials. Then, powders are blended for the desired alloy design to fulfill the final properties. The third stage of the powder metallurgy route is to consolidate the mixed powders for the desired final shape. Then, sintering treatment is done to bond the powders together. The final stage is the application of the secondary operations for the needed final characteristic of the powder metallurgy parts [2].

One of the reasons that why powder metallurgy is preferred to other metal working processes is mainly lower manufacturing costs [1]. Beside this, ability to process complex shaped parts and close tolerances and good surface finish obtained are the other main advantages of powder metallurgy with respect to other manufacturing techniques. However, there are several certain limitations on the use of powder metallurgy as production method. The biggest disadvantage is that the powder metallurgy process is more feasible and economical with mass production of the parts. Another disadvantage for some components is that the products have porous structure that mechanical properties can be affected negatively [2].

Sinter hardening, is an innovative manufacturing method among powder metallurgy applications, which provides single step and low cost process. For high strength PM parts, a martensitic structure is needed. A secondary heat treatment step, generally oil quenching, is necessary for sintered parts to obtain martensitic structure in traditional powder metallurgy. Sinter hardening applications eliminate the necessity for a secondary heat treatment step. Due to this reason, sinter hardening has a good manufacturing economy by providing one step process. In sinter hardening, parts are cooled immediately after the sintering process in the same furnace during process cycle. Cooling is done by blowing a gas mixture to the system and the cooling rate can be adjusted by the flow rate of the gas mixture. Sinter hardening process offers combination of high mechanical properties and low cost production due to the elimination of the secondary heat treatment after sintering [3].

In the literature, there is limited study on sinter hardening of Astaloy 85 Mo powder. Astaloy 85 Mo is a prealloyed ferrous powder which contains 0.85% Mo (balance Fe). Powder mixes are prepared by admixing with 0.8% C (Graphite UF4) and different amounts of Cu. Astaloy 85 Mo powder is not produced for sinter hardening process. Astaloy powder grades are basically used in as-sintered condition with

addition of Cu and/or Ni. Investigation of the sinter hardening characteristic of copper added Astaloy 85 Mo powder is the main purpose of this study.

In this study, the effect of cooling rate and the amount of copper in the microstructural and mechanical properties of Astaloy 85 Mo will be investigated. Cu is an important additive in powder metallurgy. The melting point of copper is below sintering temperature and copper becomes liquid during sintering cycle. It enhances the as sintered densities of the products. Also, Cu improves hardenability behavior of steels by shifting the TTT diagram to the right which may increase the amount of martensite in sinter hardened parts. Both these effects can improve the final mechanical properties. In this study, three different powder mixtures namely: Astaloy 85 Mo (Fe - 0.85% Mo) with 0% Cu and 0.8%C, Astaloy 85 Mo (Fe - 0.85% Mo) with 1% Cu and 0.8%C, Astaloy 85 Mo (Fe - 0.85% Mo) with 2% Cu and 0.8%C are investigated. The effect of final microstructure on mechanical properties of the specimens is evaluated.

The following chapters include literature review and theory, experimental procedure, results and discussion sections. Firstly, basics of powder metallurgy, sintering theory, sinter hardening studies and effect of sintering parameters and alloy design will be revealed in the literature review and theory chapter. After that, experimental procedure applied in this thesis study will be detailed. Then, the mechanical test results and characterization results will be given in details in the fourth chapter. Finally, the results and literature review will be discussed.

CHAPTER 2

LITERATURE REVIEW AND THEORY

Ferrous powder metallurgy has been effective and alternative way of metal part production method due to its lower manufacturing cost when compared with other routes such as; machining, casting and other similar manufacturing ways of ferrous metals [1].

There are several advantages of powder metallurgy when compared to other manufacturing techniques. Powder metallurgy is an environmentally friendly process and enables complex shape production as a near net shape process. Close tolerances, better dimensional accuracy and good surface finish are attainable in powder metallurgy method. Almost all of the income raw material is used in powder metallurgy. As a consequence, there is no waste as scrap in this manufacturing technique. Materials which are difficult to process with other production ways can be put into service for the usage of human being with the help of powder metallurgy. Manufacturing of some parts i.e. some carbides, self-lubricated bearings and super hard cutting tools can be convenient only with powder metallurgy. The parts with different chemical compositions, porous structures and the alloys which have poor casting capability can be easily produced by powder metallurgy. Various material properties; for instance, purity, density, porosity and particle size can be under strict control in this production technique. Powder metallurgy provides high production

rates due to the mass-production techniques. The products of powder metallurgy are highly pure and have longer service life [2]. Powder metallurgy comes up as an effective manufacturing technique for certain applications when these advantages are considered, but there are also several limitations of powder metallurgy. Powder metallurgy become economic with mass production because the cost of the powders is high; as well as, the tools and dies for production setup are expensive. The products of powder metallurgy are generally porous. The flow of the powders is lower than liquid metals and this difference creates a porous structure in material [2]. Porosity sometimes may be a need for some special applications but it generally affects the material properties negatively and it may commonly transform into a disadvantage.

The largest market in the world for the ferrous powder metallurgy is automotive industry (Figure 1) [1].

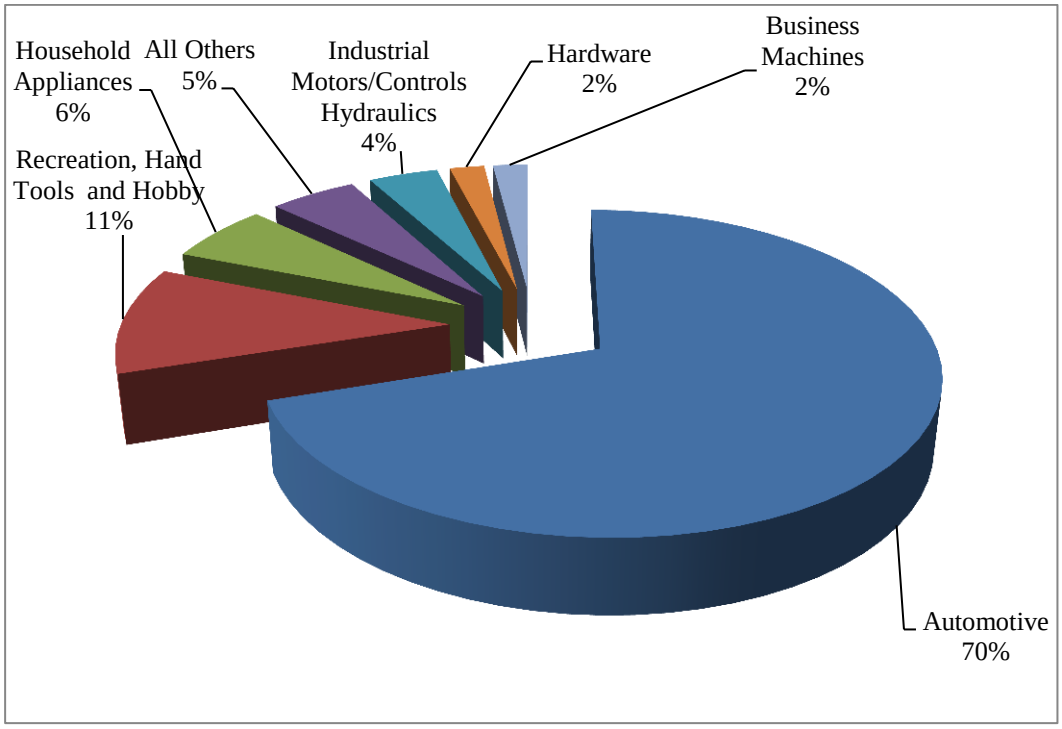

Figure 1: Application areas of powder metallurgy and the market distribution over industries [1].

2.1. Powder Production

Almost all materials can be turn into powders. As well, the manufacturing method of powders has a great impact on specific material properties of the metal parts that produced by these powders [4]. The size and the shape of the powders affect the properties and characteristics of the metals. Therefore, metal powders with different physical and chemical properties can be manufactured by the various fabrication methods which are mainly categorized as mechanical communition, chemical reaction, electrolytic deposition and atomization [2].

2.1.1. Powder Production by Mechanical Communition

Mechanical fabrication techniques of the powders can be classified into four fundamental processes: impaction, attritioning, shearing and compression. Impaction process occurs by blowing of a material and this creates cracks and causes reduction in size of the particle. Attritioning reduces the size of the particle by rubbing action. Shearing breaks the material by cleavage type of fracture with the help of cutting. Shearing process is applicable when the material is not extremely hard and the powders produced by shearing are generally coarse. Production of the powders by compressive forces has a principle of manufacturing by breaking the material. The idea behind the compression process is that the material which powder is produced from should be brittle and the powders generated by this process are coarse. Machining and milling are generally used for mechanical communition in production of powders [4].

2.1.2. Powder Production by Chemical Reactions

Powders can be manufactured by chemical reactions which consist of chemical reduction and chemical decomposition process. Chemical reduction is an efficient way to produce metal powders from metal compounds. Metals can be produced by reduction under H_2 or CO in an atmosphere controlled furnace at a temperature below the melting point of the product. After reduction process, crushing and milling is applied to the reduced product to obtain metal powders. Copper, molybdenum, tungsten and nickel powders are generally preferred to be manufactured in reduction process due to its lower cost and convenience [2]. Another way of powder production is chemical decomposition process. Decomposition process can be classified under two categories: decomposition of metal carbonyls and decomposition of metal hydrides. The most widespread examples of metal carbonyls decomposition are iron and nickel powder production. The carbonyls have a low boiling point and they are liquid at normal temperatures. The formation of carbonyls takes place by reaction of the metals and carbon monoxide gas under pressure. To decompose the carbonyl group, the vapor is heated under atmospheric pressure. In order to obtain metal powders, decomposition process should be occurred in the gas phase, not in the surface of the reaction vessel [5]. By this process, metal powders can be generated from carbonyl groups by chemical decomposition. Metal powders can also be produced from hydrides by chemical decomposition. Metal hydrides are stable at room temperature and they are reasonably brittle [2]. This characteristic of the metal hydrides enables the milling of the metal hydrides into powder form in desired fineness easily. After that, metal hydrides in powder form should be decomposed to obtain metal powders. Decomposition occurs by heating the hydride powders in a vacuum atmosphere at the same temperature which hydration takes place. During decomposition of the hydrides, the most important point is to avoid contamination of O_2, N_2, and C. By this method, refractory metals like titanium, zirconium, vanadium, thorium, uranium and high hardness metals like tantalum, niobium can be produced [5].

2.1.3. Powder Production by Electrolytic Deposition

Powders can be manufactured by electrolytic deposition. Under certain cases, there is powder precipitation at the cathode of an electrolytic cell. Firstly, the anode dissolution takes place under an applied voltage in an electrolytic cell. There are both reactions at the anode and cathode and electron transfer due to the reactions. The aim of the transport through the electrolyte is to purify the powders which are precipitated at the cathode. Deposited powders are removed from the cathode, ground into the desired fineness and heat treated to remove strain hardening. The main advantage of electrolytic deposition method for powder production is that the produced powders have high purity. For this reason, electrolysis method is generally preferred for palladium, copper, iron, zinc, manganese and silver powder production [4].

2.1.4. Powder Production by Atomization

Another procedure for powder production is atomization which is mainly formation of the powders by very rapid solidification of the liquid metal and fragmentation into metal powders. In this powder production method, liquid metal comes out of a small orifice and the liquid metal is disintegrated by a jet which blows compressed air, inert gas or water. The disintegrated small liquid particles solidify rapidly [6]. Elemental and prealloyed powders can be produced by atomization method. Applicability of atomization process to several alloys and easy process control of atomization are the main advantages of atomization process when compared to other powder production techniques. Basics of atomization rely upon fusion technology which procures tight control over alloy design and purification of the melt. Atomization process differs according to the type of the jet used for the process; in terms of, gas atomization and water atomization. The operation parameters for gas atomization including gas type, residual atmosphere, melt temperature, melt viscosity

when enters the jet nozzle and gas temperature are very important to control the process and design tailor made powder characteristics for different usages. The product in gas atomization method is homogeneous and has a great packing ability due to its spherical shape. The most common technique for production of elemental and alloy powders from metals is water atomization method if the melting point is below approximately 1600^{o}C. Water atomization is a more rapid solidification process when compared to gas atomization. There are critical differences between gas and water atomization methods due to rapid solidification of the powders. The water atomized powders have an irregular and rough shape with some oxidation at the surface of the powders because of rapid cooling. The powders produced by water atomization have a chemically heterogeneous character because there is limited chemical segregation within an alloy particle due to rapid solidification of the particles. The particles have irregular and nonspherical structure with oxidation layer at the surface of the powders. For better control of powder shape and oxidation, synthetic oil and non-reactive liquids can be preferred instead of water [4].

2.2. Alloying Methods in Powder Metallurgy

The aim of the secondary heat treatments in powder metallurgy process (which is generally quench hardening and tempering) is to improve specific material properties like toughness and hardenability. Hardenability is the ability of a material to form martensitic microstructure during furnace cooling. As well as, alloying element additions affect the hardenability of the materials and the procedure of alloying element additions has a different impact on microstructure of the material and size, distribution and shape of porosity which affects the mechanical properties of ferrous powder metallurgy products directly. Methods of adding alloying elements to the pure metal varies in powder metallurgy process when compared to other production techniques. There are several alloying methods in powder metallurgy; namely,

admixing, diffusion alloying (partially prealloying), prealloying and hybrid methods as shown in Figure 2.

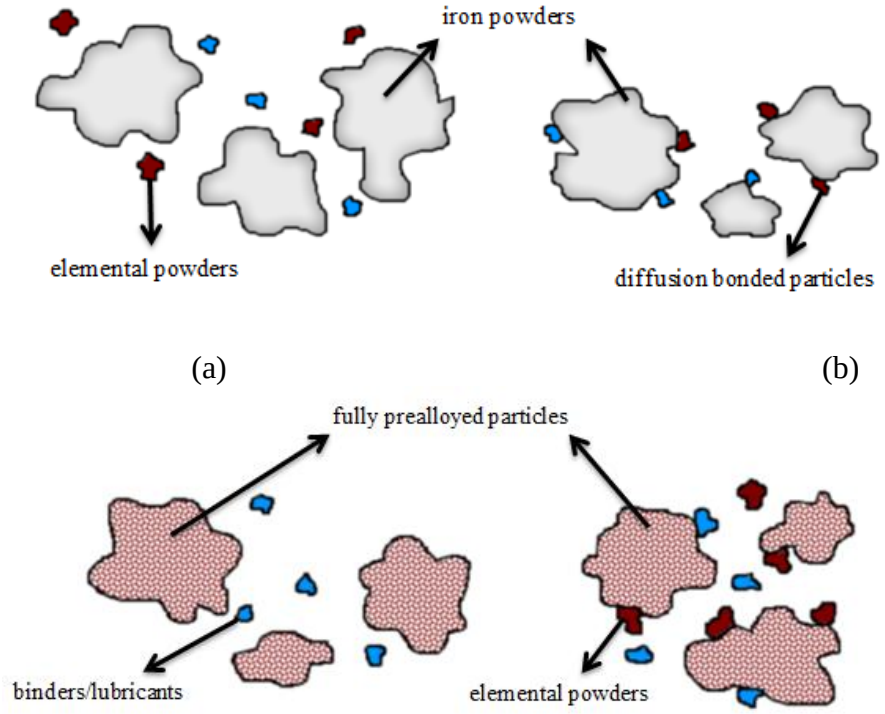

Figure 2: Schematic view of alloying mechanisms in powder metallurgy a) admixing b) diffusion alloying c) prealloying d) hybrid alloying

2.2.1. Admixing of Powders

Admixing is a conventional alloying method which is applied by adding alloying elements in elemental powder form to pure iron powder. Admixing is the most common alloying method due to its lower cost when compared to other alloying methods. In this alloying method, pure iron powders and alloy powders are mixed physically, but there is no chemically mixing in this way of alloying. As well as, the sintering temperature is not so high to give an opportunity for diffusion of alloy powders and iron powders. From this point, alloying by admixing does not give a chemically homogeneous structure. This property causes powder segregation.

2.2.2. Diffusion Alloying of Powders (Partially Prealloying)

Diffusion alloying (partially prealloying) is another process for alloying in powder metallurgy process. The base powder and elemental alloying elements in powder form are annealed together to bond alloying powder to base powder [7]. The alloying powders move to the powder boundaries of the base powder during annealing and create interparticle bonds between the base powder and alloying powder at the base powder boundaries which become highly alloyed regions in a network structure. This situation causes heterogeneous microstructure. Diffusion alloyed powders are generally highly compressible because compressibility of the base powder is generally retained after diffusion alloying [8].

2.2.3. Prealloying of Powders

The other method of alloying in powder metallurgy is prealloying. Prealloying is done by adding alloying elements to the molten metal before atomization process [7]. Uniform distribution of alloy content to each particle can be provided after atomization by prealloying process because chemical composition of each particle is same [9]. In the light of this information, homogeneous microstructures can be achieved by prealloying of the powders. On the other hand, compressibility of the prealloyed powders is lower when compared to admixed or diffusion alloyed powders due to the uniform structure of alloying elements in the particles [8].

2.2.4. Hybrid Alloying of Powders

Hybrid method is a combination of previously mentioned three methods. All methods have different significant advantage and also disadvantages. Hybrid method is generally used for optimization of the specific property of final structure such as,

hardenability and compressibility. Generally, hardenability of the prealloyed powders is higher than admixed or diffusion alloyed powders. On contrary, admixing or diffusion alloying is more beneficial when compared to prealloying in terms of high compressibility. Hybrid method seems to be a solution for this optimization problem by combining prealloyed powders with admixed or diffusion alloyed powders [8]. The base powders used for the sinter hardening process is generally preferred as prealloyed powders due to homogeneous and uniform nature of alloy content in the system. However, some other alloying elements i.e. carbon in the form of graphite and copper are generally added to the system by admixing in most of sinter hardening applications because adding such alloying elements to the base powder by prealloying has generally detrimental effects on both green strength and compressibility [9].

2.3. Compaction of Powders

Powders generally behave like fluids and this character gives an opportunity to shape under wide range of stresses [10]. The aim of compacting is to convert the loose powder into a green body with desired shape and size. There are several methods that can applied for compaction of powders; namely, pressing, centrifugal compacting, slip casting, extrusion, gravity sintering, rolling, isostatic moulding and explosive moulding [6]. The most common method for metal powder compaction is pressing of the powders. In pressing, the powders are compacted in a die having an accurate shape and size with the help of pressure. The cavity in the die has the shape of the desired final product. Metal powders are placed into the die cavity and pressing is done by with the help of punches that press the powders from top or bottom or both [2]. Mechanical press machines are preferred for pressing at low pressure while hydraulic press machines are selected for compacting at high pressure [6]. The pressure which is applied to the punches should be uniform to have a uniform compressibility of the powders and should be high enough to press powders and attain a mechanical bonding between powders which called as cold welding. After

compaction, compacted parts in desired shape and size have a specific green density and green strength by the help of cold welding that occurs between powder grades. However, these achieved green strength and green density is not high for the use of its application, these green properties of the material is only useful for handling of the part. To improve these specific properties, sintering should be done to fulfill the property requirements of the parts [2].

2.4. Sintering of Compacted Powders

Shaped powders after compaction process have incomplete strength when the desired final mechanical properties of the powder metallurgy products are considered. There is a certain need for a firing treatment called as sintering to meet the desired criteria because bonding of the powders with the help of sintering is an obvious necessity to fulfill the final properties of the parts. This is why sintering treatment is so important in the powder metallurgy processing route [10]. Sintering is a treatment which helps powders to chemically bond each other at elevated temperatures for forming a coherent and solid structure [5]. Sintering treatment forms interparticle bonds between powders which reduce surface area of the particles during sintering. As well as, reducing surface area of the powders lowers the surface energy of the powders by sintering treatment. These interparticle bonds are done by diffusion mechanisms at the atomic level [10]. Sintering generally can be classified in two main types; namely, solid state sintering and liquid phase sintering. When the powders are sintered in solid state at the sintering temperature, it is called solid state sintering. If there is a liquid phase in the compact at the sintering temperature, liquid phase sintering mechanism occurs. Beyond these types of sintering, there are also different sintering mechanisms as sub-groups, namely; transient liquid phase sintering, viscous flow sintering and activated sintering [11]. For many metals, the interparticle bonds are created by solid state diffusion. Solid state diffusion does not take place alone if one of the alloying elements in the compacts melts below sintering temperature. In this case, liquid phase sintering is also effective on diffusion mechanisms beyond

solid state diffusion due to the reason that there is a liquid-solid mixture during sintering cycle. The liquid phase present in the thermal cycle creates a capillary force which influences the rate of mass transport resulting better bonding and different properties in comparison to solid state sintering [10].

2.4.1. Solid State Sintering

Sintering is a very complex process due to the reason that there are different stages in terms of driving forces and material transport mechanisms involving in the stages of sintering. Solid state sintering mainly consists of initial, intermediate and final stage of sintering. The stages can be summarized as:

1- Initial bonding among particles
2- Neck growth
3- Pore channel closure
4- Pore rounding
5- Densification or pore shrinkage
6- Pore coarsening [5].

The driving force for sintering is the excess surface energy of the powder when compared to a fully dense material [12]. In solid state sintering, the driving force is reduction of total interfacial energy by the change in interfacial area and the change in interfacial energy [11]. Sintering is a thermal treatment and formation of the bonds between powders is achieved with the help of this thermal energy input since atomic transport mechanisms are significantly influenced by elevated temperature. Formation of bonds between particles occurs in the initial stage of sintering. While the powders are getting attached to each other in the initial stage, the neck is formed between particles to decrease surface energy. Formation of the neck is the most important event during initial stage in terms of driving force. The growth of the neck continues during the intermediate stage of sintering and causes large amount of

shrinkage in the intermediate stage. Channels between pores start to close off due to shrinkage which means that the compacts begin to become more dense during intermediate stage of sintering [12]. The main driving force during intermediate stage is the change in the interfacial energy due to densification [11]. With the help of neck growth and shrinkage in the intermediate stage of sintering, irregular shaped pores start to become rounded and they shrink due to the atomic motion to the pores to decrease surface energy [12]. In the final stage of sintering, grain growth and pore removal occur to increase densification but sintering time is very important to prevent growth of the pores during last stage of sintering because retained pores can grow at longer sintering time to balance their internal pressure [13]. The driving force for the final stage of the sintering is the change in interfacial area due to grain coarsening [11].

2.4.2. Liquid Phase Sintering

Liquid phase sintering takes place with the presence of a liquid phase in the compact during all or a part of the sintering cycle to enhance densification by spreading the liquid phase to the pores and grain boundaries with the help of capillary forces. Liquid phase sintering consists of the main stages which overlap each other, namely; rearrangement, dissolution-precipitation and solid state sintering [5]. Liquid phase sintering results in faster sintering due to faster atomic diffusion than solid state sintering. Wetting liquid creates a capillary attraction, as internal force over solid particles, which influences rapid compact densification. The liquid phase present in sintering helps rapid rearrangement of the solid particles by reducing interparticle friction. Furthermore, liquid phase dissolute at the sharp particle edges and corners and allow decrease in porosity content by creating a more efficient packing. In the first stage of the liquid phase sintering, the compact is heated to sintering temperature where the liquid phase is formed due to its lower melting point than sintering temperature. By the formation of wetting liquid on the solid particles, rapid

initial densification starts by the means of capillary forces. As well as, the system tries to minimize its surface energy by decreasing the porosity content. The compact behaves like a viscous solid as a respond to internal forces due to capillary action during rearrangement stage. Viscosity of the compact increases with the elimination of the pores and the densification rate decreases as a result. In the beginning of the rearrangement stage, the kinetics of rearrangement are very fast and rapid but as densification by rearrangement stage starts to slow down by increase in the viscosity of the compact, effects of solubility and diffusivity mechanisms become more dominant and important in the second stage of the liquid phase sintering. The second stage is called as solution-reprecipitation. Solution and reprecipitation stage is figured by microstructural coarsening. In the first stage, grain boundaries are surrounded by the liquid phase present in the compact. In addition, the small grains have higher solubility than coarse grains which creates a concentration gradient in the liquid phase. Transportation of atoms from smaller grains to larger grains by diffusion happens due to this concentration gradient. The process which causes the growth of the larger grains and the elimination of the smaller grains is termed as coarsening or Ostwald ripening. Solution and reprecipitation stage results in grain coarsening and densification. Moreover, the second stage of the liquid phase sintering allows grain shape accommodation to reduce porosity content. The shape of grains can be changed by diffusion for better packing of the grains which leads to densification by pore elimination and decrease in interfacial energy. In the last stage of liquid phase sintering, solid state mechanisms are dominant and densification rate is very slow due to the presence of solid structure in the compact. Being that the rate is very slow, solid state sintering is not so efficient in the sintering cycle in terms of densification. Solution- reprecipitation, coalescence of the grains or solid state diffusion can lead to the diffusion events in the final stage altogether [13]. There are also different types of liquid phase sintering; namely, viscous flow sintering and transient liquid phase sintering. If the liquid content in the compact is very high, viscous flow sintering occurs. In viscous flow sintering, densification is almost fully achieved by viscous flow of grain-liquid mixture and there is no grain shape accommodation stage during densification in viscous flow sintering. Transient liquid

phase sintering combines liquid phase sintering and solid state sintering. In this process, liquid phase involves in action only at the beginning of the sintering process. While sintering cycle continues, the liquid phase disappears and the most of the densification is completed by solid state sintering [11].

2.4.2.1. Activated Sintering

Activated sintering is a process which is applied to lower the activation energy for sintering [5]. Lowering the activation energy for sintering can supply a lower sintering temperature, shorter sintering time or better final properties in the same sintering conditions. Different methods varying from adding chemicals to the system to applying external electrical fields to the system are done to lower the activation energy needed for sintering [4]. The most common method for activated sintering is chemical additions as activators to the system which forms with the base powder an eutectoid liquid which have a melting point below sintering temperature [14]. There are some criteria for chemical additions. A metal or compound which is added to the system as an activator must have lower melting point than sintering temperature. Furthermore, the base metal should have a low solubility for the added chemical compound or metal while the activator should be highly soluble in the base metal. As well as, the activator segregating between interparticle interfaces should stay in the interfaces during sintering cycle [4].

2.5. Sinter Hardening

Generally, the compacted powders need secondary heat treatments to improve their mechanical properties after sintering stage. Therefore, the secondary heat treatments that applied to compacts after sintering can be called as hardening stage of the powder metallurgy parts. Sinter hardening is a process that combines sintering and

hardening stage step by step in one operation in the same sintering cycle [15]. There are several advantages of sinter hardening over conventional Q&T (quench and tempering). The main advantage of sinter hardening is its economic nature. It is a cost reducing process. In industrial operations of powder metallurgy, continuous mesh belt furnaces are used for sintering to fulfill the need for mass production. The sintered parts, come out of the continuous mesh belt furnace, need secondary heat treatment which is generally oil quenching to improve mechanical properties by attaining bainitic and/or martensitic microstructures. The sense in the sinter hardening is to smooth the way of hardening process by combining sintering and hardening in the same continuous mesh belt furnace. After sintering in the same continuous mesh belt furnace, the hardening stage occurs by flowing gas mixtures and/or air to a separate part of the furnace with a certain flow rate which causes fast cooling of the sintered parts. Elimination of the secondary heat treatments and preventing time losses results in cost reduction. The elimination of quench hardening treatment supplies other critical benefits such as easiness to tempering treatment, reduction in distortion of the parts. The powder metallurgy products have a porous structure and oil contamination of the pores is a big problem during oil quenching. Oil quenched products definitely need oil removal process after quench hardening treatment when sinter hardened parts do not need any further operation. Oil contamination also affects tempering treatment which generally applied after hardening stage to improve toughness of the parts. If tempering is done at temperatures over 200 ^{o}C, the quench hardened parts have to be tempered firstly under 200 ^{o}C to sweep away the oil contamination in the porous structure and then tempering can be done after this oil removal process. From this point of view, tempering for sinter hardened parts is much easier than quench hardened ones [8]. Quenching also leads to surface cracks and dimensional changes in the parts. Sinter hardening is an attractive method for better dimensional control due to the reduction in distortion in the parts.

2.6. Variables Affecting the Final Properties of Powder Metallurgy Products

The aim of the powder metallurgy is to produce products with desired mechanical properties by designed microstructures. The way of achieving the designed microstructures is to control the variables which affect the final properties of the products [11]. Improved mechanical properties of the powder metallurgy products can be provided by microstructural control which is directly affected by manufacturing conditions and material selection. A microstructure consists of bainite and martensite is desirable for high strength applications [16]. Microstructural control can be attained by controlling both manufacturing conditions and material selection.

2.6.1. Manufacturing Conditions

Manufacturing conditions are critical for the final products. The process variables affecting the final properties are mainly sintering conditions and heat treating conditions [17].

2.6.1.1. Sintering Conditions

Sintering stage is very crucial in terms of desired final properties. The factors affecting the microstructure are mainly sintering temperature, sintering time and sintering furnace atmosphere [5].

2.6.1.1.1. Sintering Temperature

Sintering is a thermal treatment which assembles the powders together and mass transport mechanisms are effective in bonding the powders together. Atomic mass transport mechanisms exponentially increase with an increase in temperature. As well as, the rate and magnitude of the mass transport events during sintering cycle increases extensively by increasing the sintering temperature [5]. As expected, the sintering temperature is an important parameter which has a significant effect on mechanical properties of a powder metallurgy steel product. Better diffusion of alloying elements is a reason of sintering at higher temperatures. As well as, better hardenability of the base powder can be attained by better diffusion of alloying elements [16]. Chagnon et. al. [18] reveals that sintering at higher temperatures increases the sintered density of the powder metallurgy products by densification process and densification enables porosity shape accommodation stage which improves mechanical properties. According to their studies, higher apparent hardness values and higher ultimate tensile strength can be attained by higher sintering temperatures, but an increase in sintering temperature has a more dominant effect on lower carbon content steels as can be seen in Figure 3. For industrial applications, there are generally limitations in sintering temperature. In powder metallurgy industry, sintering is widely done in continuous mesh belt furnaces which operate at 1120^{o}C-1150^{o}C. Higher sintering temperatures are beneficial for homogenization of the alloying elements but such high temperatures are not beneficial for economic reasons. In addition, continuous mesh belt furnaces used in powder metallurgy industry cannot be used above 1150^{o}C due to the limitations in the material used for furnace construction [17].

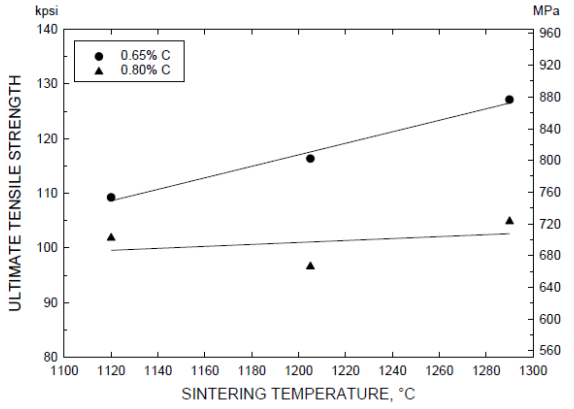

(a)

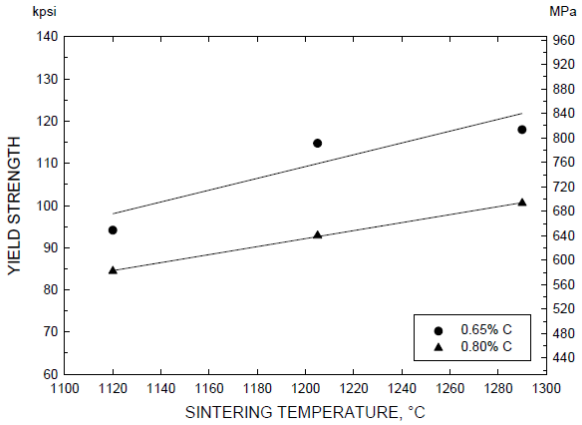

(b)

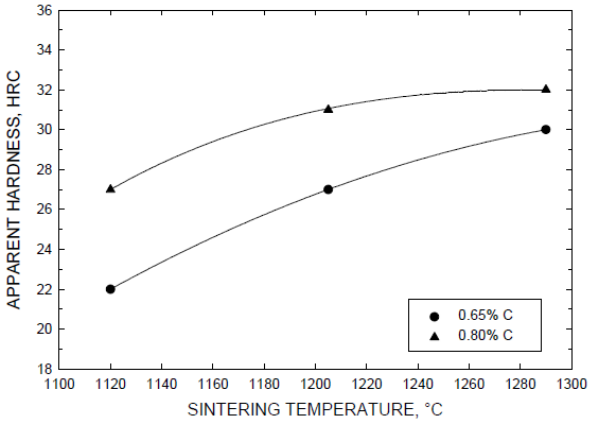

(c)

Figure 3: Effect of sintering temperature on mechanical properties: a) ultimate tensile strength, b) yield strength, c) apparent hardness [18].

2.6.1.1.2. Sintering Time

An increase in sintering time influences sintering and allow for mass transport mechanisms. The studies of Nyberg et al show that sintering necks are not well developed for shorter sintering times [19]. As Kang et al revealed in their study, densification process is enhanced with longer sintering times which can be seen in Figure 4 [11]. However, effect of longer sintering times is small when compared to the effect of the increase in sintering temperature because mass transport mechanisms are mainly influenced by temperature. As well as, it is difficult to attain a fully dense material with longer sintering times at any temperature because there is a loss in terms of driving force of atomic mass transport mechanisms [5]. Moreover, increasing sintering time increases also surface decarburization and causes lower hardness [19].

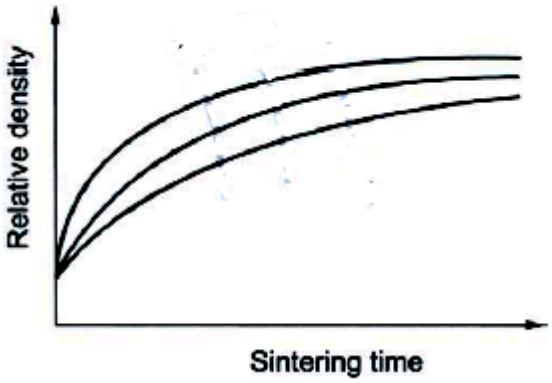

Figure 4: Effect of the increase in sintering time on sintered density [11].

So much longer sintering times are not effective on mechanical properties of the powder metallurgy products and there are some problems with longer sintering times as mentioned previously. Therefore, there can be optimization between sintering time and sintering temperature by using not so long sintering times and not so high

sintering temperatures with respect to the cost of the sintering process [5]. In industrial applications, sintering cycle is generally selected as maximum 30 minutes for economical reasons [17].

2.6.1.1.3. Sintering Furnace Atmosphere

The sintering atmosphere is very critical for desired final properties. The first criterion of a good sintering atmosphere is to protect the powder compact from oxidation during sintering cycle. As well as, the atmosphere should reduce the residual surface oxides to improve the interfacial contacts between particles during sintering. The second important criterion is that if the compact contains carbon, the furnace atmosphere should protect the compact from decarburization. There are some common protective atmospheres for iron powder metallurgy; namely, reducing-carburizing atmosphere (i.e. endogas), reducing-decarburizing atmosphere (i.e. hydrogen, cracked ammonia) and neutral atmosphere (i.e. nitrogen) [17].

2.6.1.2. Heat Treating Conditions

Increase in the mechanical properties of the powder metallurgy products is directly related with the microstructure which can be controlled by post sintering cooling rate [19]. The microstructure of the sintered parts can be altered to attain the required content of martensite to fulfill desired properties by changing the post sintering cooling rates [20]. To achieve the microstructure needed for final properties, different heat treatments can be applied during or post sintering cycle; such as, quenching or sinter hardening. The cooling rates of several processes can be seen schematically in Figure 5 on a continuous cooling diagram of an alloy steel [21]. Additionally, the cooling rate of sinter hardening treatment can be modified by changing the flow of the compressed air or gas.

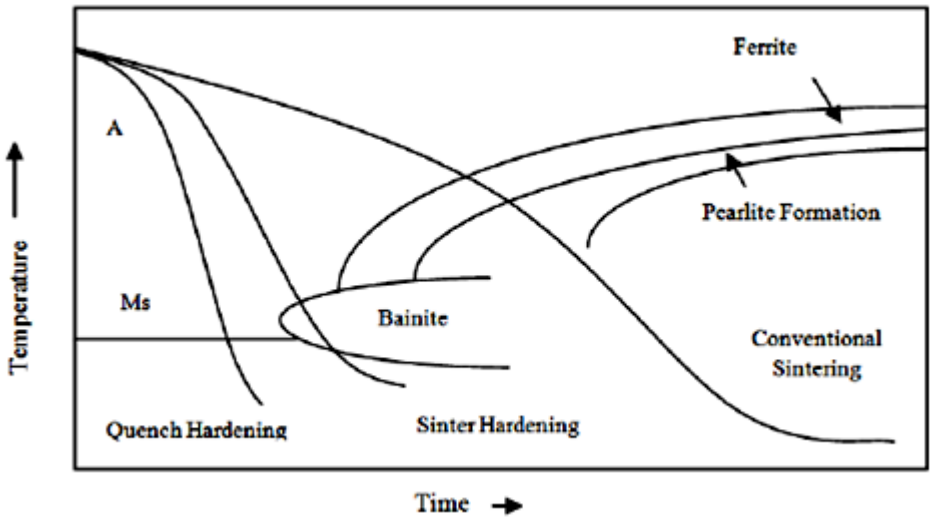

Figure 5: Schematic continuous cooling diagram of an alloy steel [21].

Engström found that post sintering cooling rate has a great effect on microstructure. It is revealed that sinter hardening with a cooling rate of 1°C/sec. results with 40% martensite and 60% bainite in the microstructure while fully martensitic microstructure can be achieved by increasing the cooling rate to 6°C/sec as seen in Figure 6 [20].

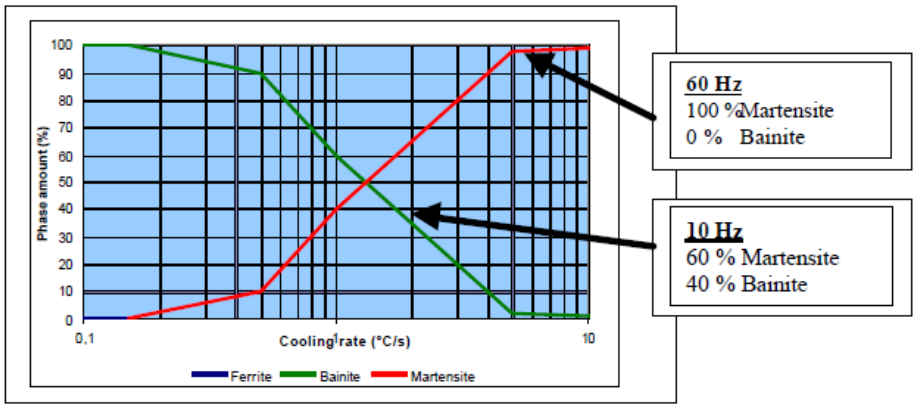

Figure 6: Effect of post sintering cooling rate on the amount phases of Distaloy DH (1.5%Mo-2%Cu-0.7%C) [20].

The attained microstructures with an increase in the post sintering cooling rates which consists of bainitic and/or martensitic microstructures result in an increase in the mechanical properties. According to the study of McLelland et al. [22], increasing the post sintering cooling rate has a greatest effect on hardness. On the other hand, there is slight change in transverse rupture strength with the increase in cooling rate as can be seen in Figure 7. The study of McLelland shows that transverse rupture strength increases when the sintering time is increased from 10 minutes to 30 minutes.

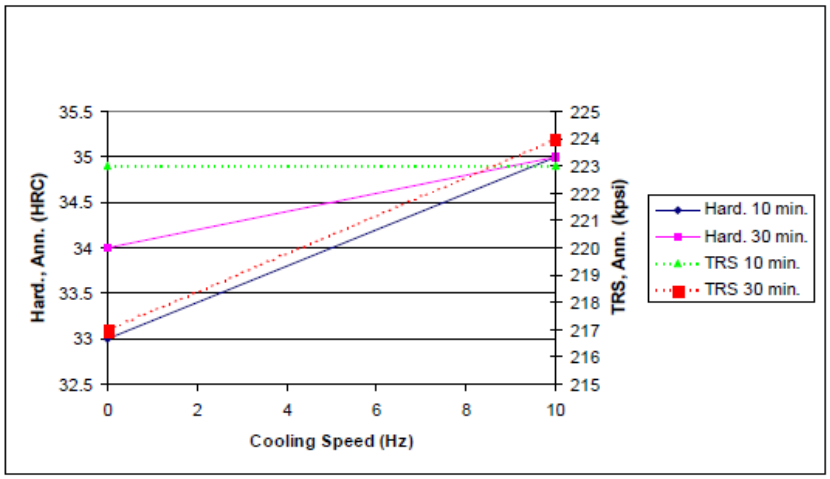

Figure 7: Effect of cooling rate on hardness and transverse rupture strength of Astaloy A powder grade (1.5%Mo-2%Cu-0.8%C) [22].

2.6.2. Material Variables

The final properties of powder metallurgy products mainly depends on the variables of the materials used in the compact; namely, particle size, particle shape, particle structure, the density and the composition of the particles.

2.6.2.1. Particle Size

A decrease in the particle size of the compact creates an option for better sintering, that is due to that interfacial areas between particles and pores increases which affects driving force for sintering significantly. Smaller particle size influences all types of atomic mass transport mechanisms by creating greater surface area which promotes more surface diffusion and creating also larger interparticle contact area which promotes more volume diffusion [5]. As a result of the usage of the smaller particle sized powders, better mechanical properties can be achieved due to better sintering and densification of the particles.

2.6.2.2. Particle Shape

The particle shape affects the ultimate properties because sintering kinetics are affected by the alteration of the particle shape. The decrease in the sphericity of the particle and/or the increase in the surface roughness of the particle influence sintering positively by leading larger internal surface area and greater interparticle contact between each particle [5].

2.6.2.3. Particle Structure

Grain size of the particles is very important to control the final microstructure of the sintered components. Finer grain structure affects sintering kinetics favorably and increases the final properties [5].

2.6.2.4. Density

Density is a vital parameter for the mechanical properties of the sintered parts. The change in density is directly related with dimensional stability of the products and dimensional stability is an important concern because powder metallurgy is a near net shape process. Density can be affected by many parameters which influence densification process during sintering. The increase in sintered density increases the tensile and fatigue strength of the sintered parts increase linearly. In addition, elongation and impact strength of the powder metallurgy products increase exponentially with increasing sintered density. The tendency in the change of the mechanical properties of sintered materials with an increase in sintered density can be seen in Figure 8 [17].

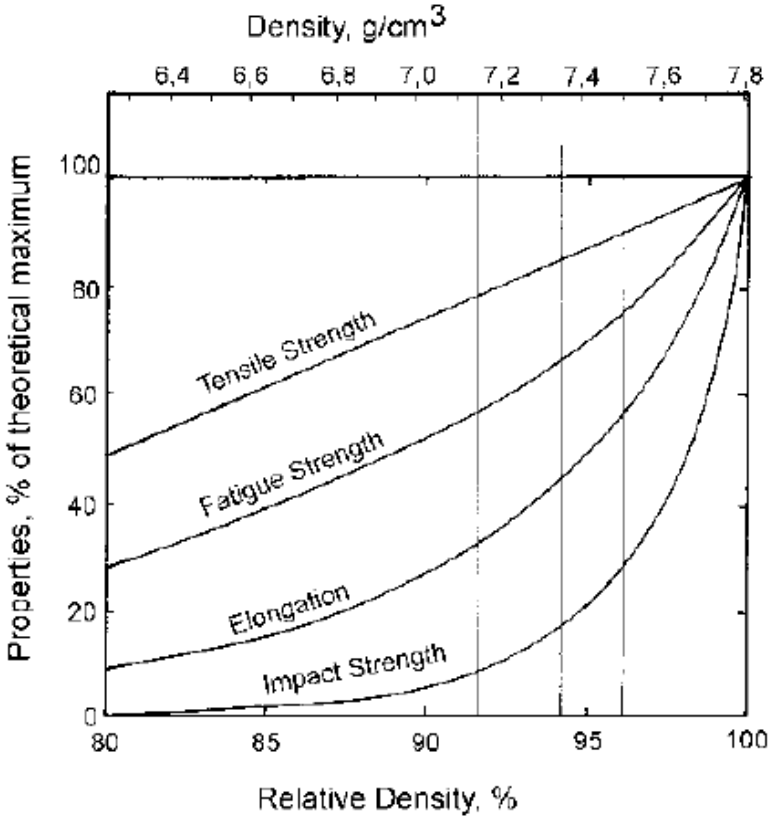

Figure 8: The change in the mechanical properties of the sintered parts with respect to increase in the sintered density [17].

2.6.2.5. Composition of the Particles

The sintering kinetics and also certainly mechanical properties of the powder metallurgy products can be affected by alloying additions or impurities within a powder metal. The impurities present in the powder compact can have beneficial or detrimental effects on the final properties with respect to the distribution of the impurities and reaction of the impurities with base material. Sintering kinetics is enhanced by dispersed phases within matrix which influence grain boundary diffusion. Impurities which cause surface contaminations are undesirable and the reaction between the matrix phase and impurities at high temperatures has deleterious effects on sintered properties [5]. Generally, effect of the alloying elements is the same for powder metallurgy steels and conventional steels [17]. The aim of the adding alloying elements to the base metal is to increase hardenability of the steel to attain desired microstructures and therefore desired mechanical properties. More clearly, the martensite content in the microstructure and hence the mechanical properties directly depend on the hardenability of the alloy and composition of the parts [18]. Additionally, highly hardenable materials do not need high post sintering cooling rates to form martensitic and bainitic microstructures. At similar cooling rates, more amount of martensite is achieved by the addition of alloying elements which increase hardenability [20]. The effect of some popular alloying elements in powder metallurgy on hardenability is shown in Figure 9 [23].

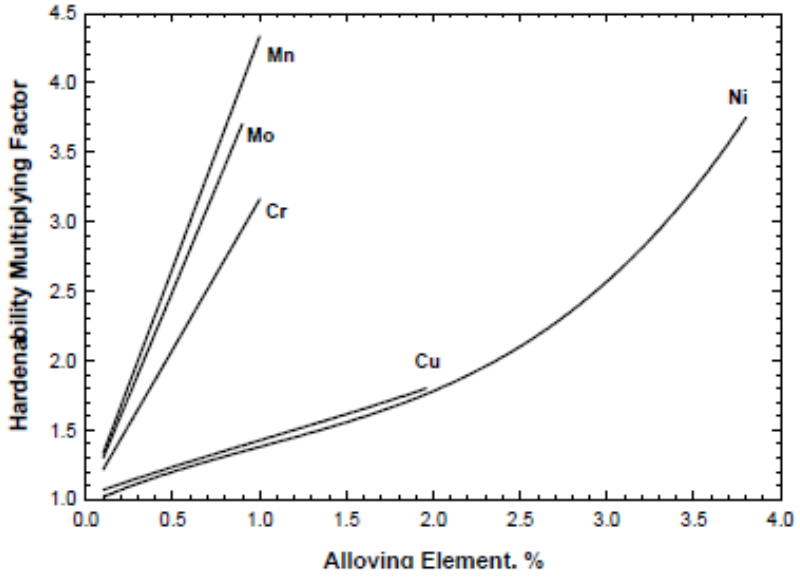

Figure 9: Effect of the main alloying elements in powder metallurgy on hardenability [23].

The desired mechanical properties are very important for structural parts, but dimensional stability should also be considered when a powder metallurgy alloy is designed for structural parts [17]. Prealloying the alloying elements has a solution strengthening effect on the ferritic matrix of the steel powders but this strengthening mechanism has a negative impact on compressibility. The effect of alloying elements on compressibility of the powder can be seen in Figure 10 [23]. While the alloy design in powder metallurgy industry is considered, there should be an optimization between the increase in hardenability and the decrease in compressibility of the powders. The higher hardenability for better mechanical properties and the better compressibility for the higher sintered density should be balanced while keeping the alloy content as lean as possible to reduce manufacturing costs [7]. Alloying elements; namely, nickel and manganese have a detrimental effect on compressibility due to their strong solution strengthening effect in ferritic matrix. Effect of molybdenum and chromium is less than nickel and manganese. Carbon and nitrogen

should be kept at very low levels to obtain compressible powders due to the reason that they form interstitial solution with iron [8].

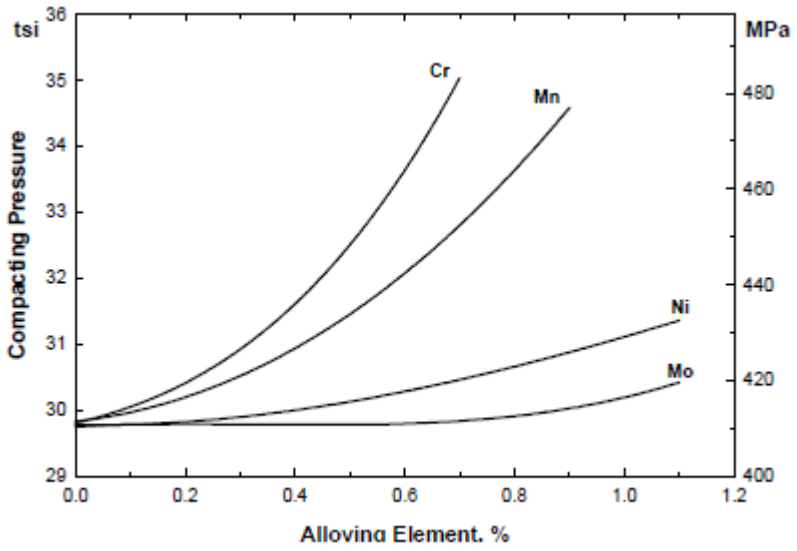

Figure 10: Effect of alloying element on compressibility of prealloyed powders admixed with 0.5%C [23].

2.6.2.5.1. Addition of Molybdenum

The tendency to use molybdenum as an alloying element in the powder metallurgy industry increases from day to day because molybdenum has a great effect on hardenability and does not affect compressibility of the powder significantly when compared to other alloying elements (Figure 9 and Figure 10). Moreover, molybdenum does not have any oxidation problem during atomization, annealing or sintering cycle [24]. Due to its advantages, usage of prealloyed powders which contains molybdenum becomes widespread for structural powder metallurgy products. If the historical advancements in sinter hardening process are investigated, it can be realized easily that the higher cooling rates could not be achieved in the early sinter hardening studies. As a result of this situation, only highly alloyed

materials were used to increase hardenability. The price of the alloying elements, especially molybdenum, increases dramatically in the recent years. As a consequence, powder metallurgy industry attracts the alloys with leaner molybdenum content [25]. From this point of view, the importance of molybdenum as an alloying element in powder metallurgy applications can be understood. Molybdenum can be added to the system as admixed or prealloyed. On the other hand, molybdenum addition by admixing is not so desirable that molybdenum diffuses into the iron matrix very slowly and the final microstructure is heterogeneous. As a result, molybdenum is generally added as prealloyed powder because homogeneous microstructures are attainable by prealloying molybdenum to the system [26]. The change in the microstructures with respect to the change in the composition of a steel can be predicted via IT diagrams of steels. Generally, post sintering treatments are not done at isothermal conditions because there is a continuous cooling from austenitization temperature to room temperature. Nevertheless, IT diagrams can still give a chance to understand the final microstructures even if the microstructures after continuous cooling may be very complex. Rutz et al. signify the effect of molybdenum on the final microstructure in their study using the IT diagram in Figure 11. The shift in the nose of the curve can be seen clearly when Figure 11.a and 11.b are compared. This shift stems from the addition of 0.24%Mo to the steel with the same composition in Figure 11.a. [3]. To say more clearly, the addition of molybdenum creates an opportunity for the transformation from austenite to martensite by shifting the pearlite nose to the right which decreases the critical cooling rate and provides a considerable time for transformation. This means that the desired martensitic microstructures can be achieved even at the lower cooling rates when molybdenum is added.

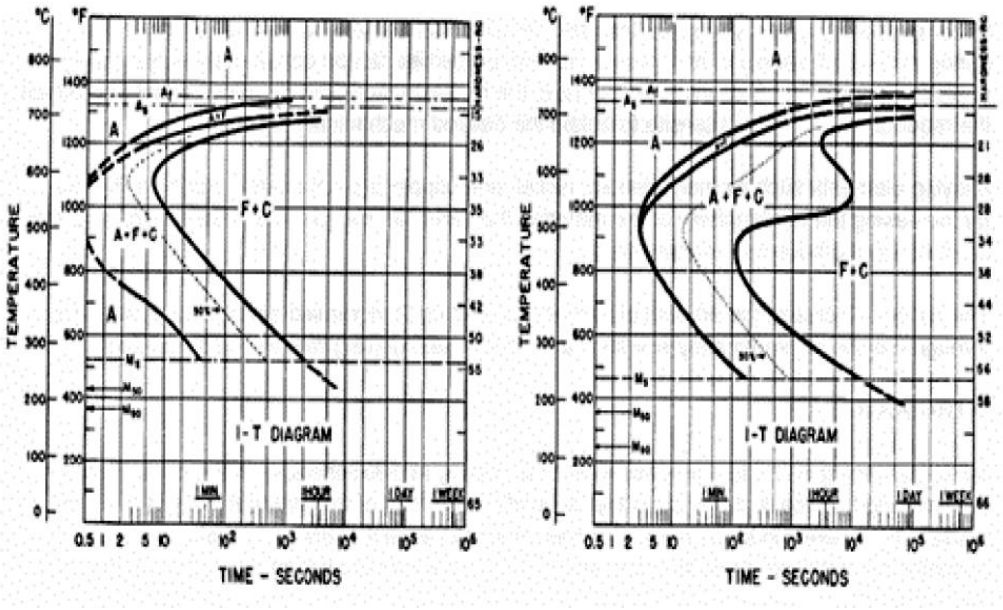

(a) (b)

Figure 11: The IT diagrams for a steel a) with no Mo b) with 0.24%Mo [3]

2.6.2.5.2. Addition of Copper

The sintering kinetics is slow at the common sintering temperatures which are 1120^{o}C-1150^{o}C and the diffusion of alloying elements is also limited at these temperatures. As a consequence, fully homogenized microstructures cannot be attained at these temperatures. The acceleration of the atomic mass transport mechanisms can be provided with liquid phase sintering [17]. The melting point of copper is 1083^{o}C and copper spreads in the iron matrix via liquid phase sintering during sintering cycle. The beneficial effect of copper on mechanical properties, its low cost and availability in the powder form makes copper as a common alloying element in the powder metallurgy industry [27]. As known, it is desired to have the largest amount of martensite in the microstructure of a powder metallurgy product and it makes the material hardest. On the other hand, sizing operations get more difficult with high hardness values. For sinter hardening applications, dimensional

control is a must. Usage of prealloyed powders with the addition of copper enables the attaining of tighter dimensional tolerances [16]. Copper is beneficial when added to the system as admixed with the base powder because compressibility and green strength decreases when copper is added by prealloying [9]. The effect of copper on continuous cooling curves of steels is discussed in 2.6.2.5.1. As well as, copper has a significant effect on hardenability as can be seen in Figure 9. As a result, increasing the copper content increases the martensite content in the microstructure and the final mechanical properties. Moreover, the addition of Cu improves hardness for only low carbon steels [28]. Effect of copper content on tensile strength and elongation with varying carbon content can be seen in Figure 12 [17].

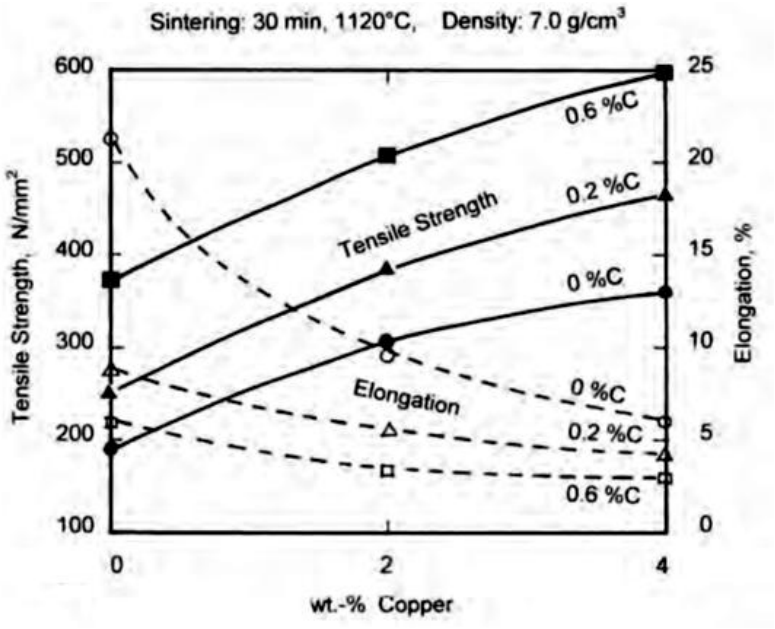

Figure 12: Effect of copper content with changing carbon content on tensile strength and % elongation on sintered iron-copper materials [17].

However, in low carbon alloys which contains copper, melt copper spreads over grain boundaries and causes dimensional swelling (growth) of the parts after sintering [23]. The growth of the parts after sintering is possible when the copper

content is higher than 2.5% copper. Carbon content is very critical to protect the compact from such a dimensional growth because carburizing effect of the carbon eliminates the risk of dimensional growth and supplies dimensional control with the appropriate graphite addition. The dimensional change with varying carbon and copper content is given Figure 13 [17]. On the other hand, when carbon and copper are admixed in the powder, the carbon content affects the diffusion of admixed copper because the atomic mass transport mechanisms of copper are restrained by the diffused carbon. In detail, the diffusion of copper at the pores and the grain boundaries is reduced by diffused carbon in austenitic regions during sintering cycle. This deleterious effect causes the formation of retained austenite in high copper regions and a higher local hardenability at pore/particle interfaces [9]. As Chagnon et al. reveal in their study that the increase in carbon and copper content results in the decrease in the martensite content in the microstructure due to the austenite formation [28].

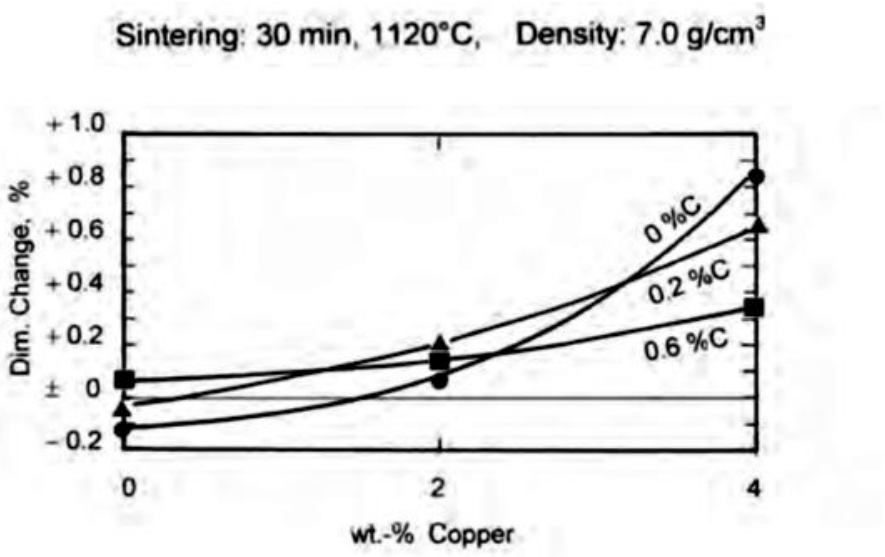

Figure 13: Effect of copper content with varying carbon additions on dimensional change after sintering on sintered iron-copper materials [17].

According to the study of Lindsey and Rutz, the addition of 2% copper to the base metal increases the properties dramatically. Lindsey and Rutz stated also that the

presence of copper and molybdenum in the system together has a great effect on hardenability of the steel which has a similar effect as an increase in cooling rate. The compacts which contain 0.5% Mo and above with the admixed 2% Cu and 0.6% C contents can be sinter hardened at a cooling rate of 1.6^{o}C/sec and 2.2^{o}C/sec. [24].

2.6.2.5.3. Addition of Graphite

Graphite is generally added to the prealloyed base powder as carbon source. Carbon is an interstitial alloying element and dissolves very rapidly in the iron matrix during sintering cycle [17]. Effect of the increase in the carbon content on the IT diagram of steels is studied by Rutz et al. [3]. As the carbon content increases from 0.47% C to 0.68% C, there is a shift in the IT curve to the as can be seen in Figure 14.a. and 14.b. In addition, there is a significant decrease in the $M_{S,}$ martensite start temperature with the increase in carbon content.

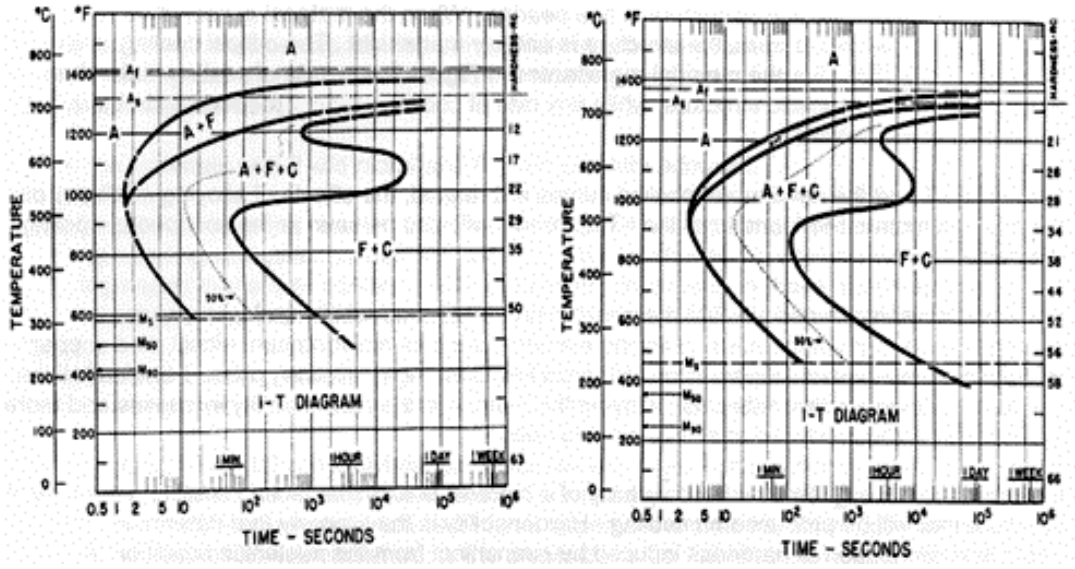

(a) (b)

Figure 14: The IT diagrams for a steel a) with 0.47% C b) with 0.68% C [3].

Even if the effect of carbon on hardenability is not as effective as the effect of alloying elements, carbon is an important element to attain high hardness in steels. The study of Chagnon et al. shows that an increase in carbon content increases the apparent hardness [18]. However, high carbon content enhances formation of retained austenite due to the reason that martensite start temperature decreases with the addition of carbon (Figure 14.a. and 14.b.) [28]. Similarly, the addition of carbon with admixed copper to the prealloyed base powder also causes an increase in the retained austenite content as discussed previously in 2.6.2.5.2. [9].

CHAPTER 3

EXPERIMENTAL PROCEDURE

3.1. Base Powder

In this thesis study, the Astaloy 85 Mo prealloyed powder is used. It is produced by Hoeganaes and generally used for as-sintered conditions. It is a water atomized powder with apparent density of 3 g/cm^3 and have a particle size range of 20-180 μm.

3.2. Powder Mixes

In this study, the Astaloy 85 Mo powder is mixed with %0.8 graphite (UF4) and different amounts of Cu. The amount of Cu is varied in the range of 0%Cu – 2% Cu. Table 1. shows the powder mixtures used in this research.

Table 1: Powder mixtures used in the research.

Base Powder	% Mo	% Cu	% C	% Fe
Astaloy 85 Mo	0.85	-	0.8	Balance
Astaloy 85 Mo	0.85	1	0.8	Balance
Astaloy 85 Mo	0.85	2	0.8	Balance

3.3. Experimental Steps

In this study, the different experimental paths are followed. The first step of experiments is mixing the base powder with the changing chemical composition of copper and %0.8 graphite (UF4). Secondly, the mixed powders are pressed into desired shape. Then, green compacts are sintered and hardened in the same sintering furnace with different cooling rates. Sintered parts are characterized by: mechanical tests, microstructural examination and porosity measurements.

3.3.1. Pressing of the Powder Mixes

The mixed powder grades were pressed under 600 MPa with Instron tension-compression testing machine in a single end die press by cold compaction. The compaction mechanism was unidirectional and velocity of the compression was 1mm/min. The samples are tested according to TS 4222 EN ISO 3325 standards for three point bending tests. After pressing, green density of the samples are found approximately 6.9 g/cm^3. Dimensions of the rectangular green compacts are 13 mm, 6.15 mm, 32.1 mm. The weight of the pressed compacts were about 17.3 gr.

Figure 15: The general view of the sinter hardened sample.

3.3.2. Sintering of Green Compacts

Sintering of the samples was done at Tozmetal Ticaret ve Sanayi A.Ş. Green compacts were sintered in a continuous belt furnace under industrial conditions. Firstly, prepared green samples were preheated to 700^{o}C for the removal of the lubricants and binders. After lubricant and binder removal, the samples are sintered under methane gas at 1120^{o}C for 20 minutes. At the end of the sintering stage, the cooling stage was started at the same continuous belt furnace. Three different cooling rates were applied: either 0.5^{o}C/sec., 1.5^{o}C/sec. or 3^{o}C/sec. Belt velocity of the furnace was 200 mm/min. and one sintering and sinter hardening cycle of the furnace was completed at 80min. The schematic sintering cycle is given in Figure 16.

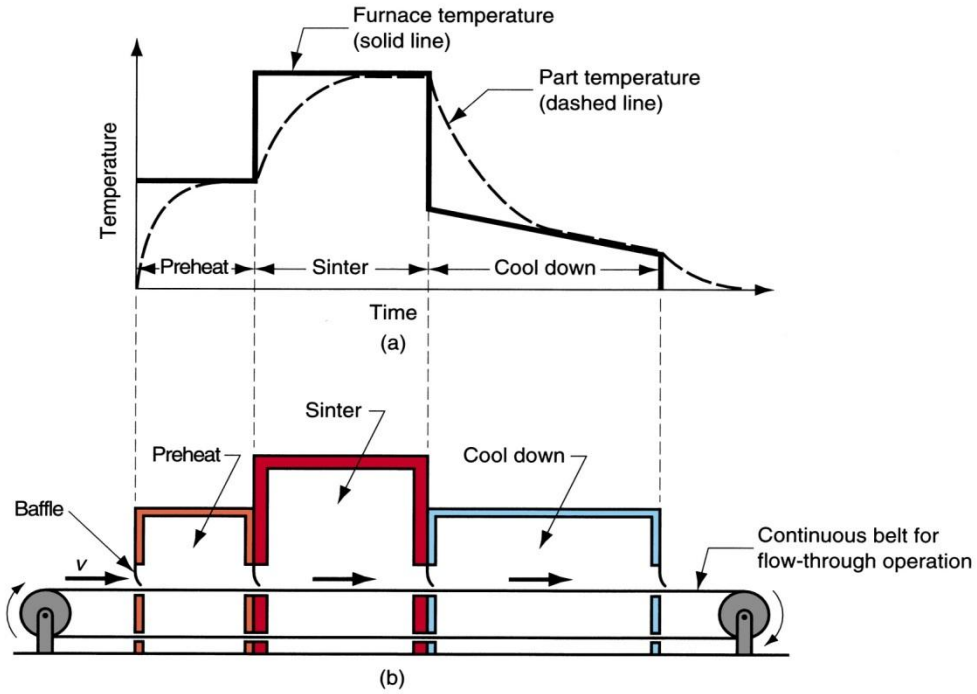

Figure 16: The schematic sintering cycle at Tozmetal Ticaret ve Sanayi A.Ş.

3.3.3. Normalizing Heat Treatment Studies

The sinter hardened samples were normalized in Proterm box type heat treatment furnace. Copper free samples and 2% Cu containing samples were used in normalizing heat treatments. Normalizing treatment was done to verify the results of microstructural characterization. Firstly, the sinter hardened samples were austenized at 850^{o}C for 10 minutes. Then, the samples were air cooled.

3.4. Characterization of the Samples

The sinter hardened samples are characterized by different stages; namely, optical microscopy, scanning electron microscopy, density and porosity evaluations and mechanical tests. The aim of the characterization is to determine the extend of sintering and attained densities.

3.4.1. Characterization by Optical Microscopy

For preparation of the specimens for optical microscopy, the sinter hardened samples are sectioned into two parts from middle along horizontal direction with Buehler Isomet 5000 Linear Precision Saw, USA. The purpose of cutting is due to obtain more representative results throughout the cross-section. After cutting, the samples are mounted into bakalite to make the sample preparation easier for easy handling of the samples. Mounted samples were grounded to achieve smooth surfaces by Metkon Gripo 2V Grinder, Turkey. After grinding, the samples were polished by firstly Mecapol P230 Polisher, France for coarse (6 μm diamond) polishing and secondly Metaserv Universal Polisher, England for fine (3 μm diamond) polishing. Powder metallurgy products have a porous characteristic and porosity can affect specimen preparation negatively. Porosity is harmful for etching step. Polishing lubricant, alcohol, or diamond particles can be embedded in porosities despite cleaning the surface of the specimen. While etching, they can come out from porosities and ruin the microstructure. The samples kept in ethanol for 24 hours and after that, the samples were cleaned by ultrasonic cleaner for 10 minutes to remove the foreign particles from the porosity. The etchant was 2% Nital solution. Different etching times were used in this study to determine the phases present and relative amount of phases in the microstructure. The optical micrographs were taken with optical microscope Olympus FMEU-F200, Japan. The amount of the present phases was

also found using the selectively etched micrographs (with 100X magnification) with Clemex Vision Professional Edition v3.5.020.

3.4.2. Characterization by Scanning Electron Microscopy

SEM studies and X-ray mapping studies are done with Jeol (JSM 6400, Jeol Ltd, Tokyo, Japan) and SEM (Nova Nano SEM 430, FEI Ltd, Oregon, USA) with EDX analyzer system. SEM micrographs of powder mixes are taken with Jeol (JSM 6400, Jeol Ltd, Tokyo, Japan) by adhering the powder mixes on carbon tape.

3.4.3. Density Measurements

Green densities of the compacts were calculated by measuring their dimensions and weights.

3.4.4. Porosity Measurements

Porosity measurements were done by quantitative methods using Clemex Vision Professional Edition v3.5.020. Porosity studies were done in as polished micrographs (100X micrographs).

3.4.5. Characterization by Mechanical Tests

3.4.5.1. Transverse Rupture Strength Test

Transverse rupture strength test is done to determine mechanical properties of the samples with Instron testing machine (capacity: 5 tons). The compression velocity is 1 mm/min. The tests are done according to TS 4222 EN ISO 3325 standards. The dimensions of the samples were approximately 12.9 mm, 6.15 mm, 32.1 mm. The mathematical expression for the transverse rupture strength can be seen in equation (3.1). After calculating the dimensions of each sample, transverse rupture strength is calculated by using this equation.

$$\sigma_B = \frac{3 \times P \times L}{2 \times t^2 \times w} \tag{3.1}$$

3.4.5.2. Microhardness Test

Microhardness tests were done by taking Vickers scale hardness values from pearlitic, bainitic and martensitic regions of the samples with Buehler microhardness intender. Vickers microhardness tests were done under 100 g. load.

3.4.5.3. Macrohardness Test

Macrohardness tests were done to detect the hardness of the samples including porous regions. The macrohardness measurements were done with Wilson-Wopert hardness machine on Rockwell C scale. The tests were done under 150 kg load.

CHAPTER 4

RESULTS

4.1. Green Density Measurements

The powder mixes, which were prepared from the base powder Astaloy 85 Mo, were cold compacted under 600 MPa pressure to attain rectangular final shape in a unidirectional die. The green density measurements of the compacts were calculated using the dimensions of the samples. The green densities of the powder mixes do not change with % Cu and yield approximately 7 g/cm^3 density (%86 - %89 of theoretical density).

4.2. Porosity Measurements

As described in Chapter 3, after a binder removal at 700^oC, the samples were sintered under methane gas at 1120^oC for 20 minutes. Three different cooling rates were applied at the end of sintering: either 0.5^oC/sec., 1.5^oC/sec. or 3^oC/sec. The porosity measurements of all the sintered specimens were done with Clemex Vision image analyzer software using optical micrographs. The pores which look black in color under optical microscope were shaded (in green) using image analyzer software as shown in Figure 17. The % porosity of the sintered samples with respect to copper

were calculated as the ratio of shaded area to total area and listed in Table 2. As shown in Table 2, the amount of porosity decreases with an increase in copper content of samples. This can be attributed to the beneficial effect of copper on sintered densities. The density measurements have shown that the rate of cooling after sintering does not affect the densities attained.

Table 2: The % porosity of sintered Astaloy 85 Mo samples with respect to copper content.

Sample	**% Porosity**
Astaloy 85 Mo – 0.8% C	12,1 ± 2,4
Astaloy 85 Mo – 0.8% C – 1% Cu	10,5 ± 2,5
Astaloy 85 Mo – 0.8% C – 2% Cu	8,5 ± 2

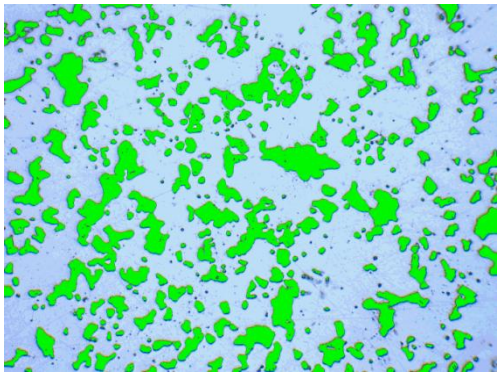

(a)

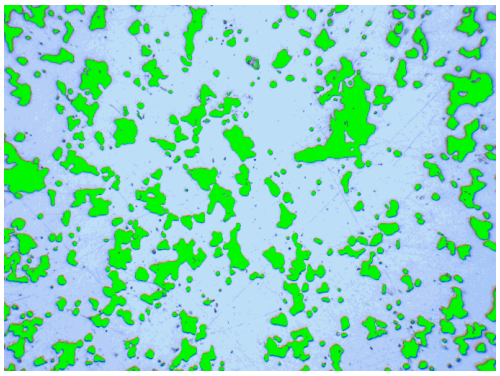

(b)

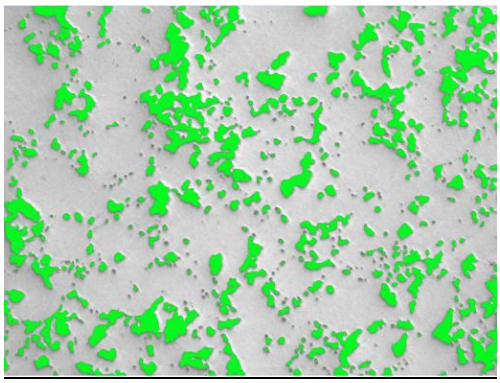

(c)

Figure 17: The pores of sintered specimens shaded by image analyzer software a) Astaloy 85 Mo admixed with 0.8 %C b) Astaloy 85 Mo admixed with 0.8 %C and 1 %Cu c) Astaloy 85 Mo admixed with 0.8 %C and 2 %Cu.

4.3. Microstructural Characterization

Sinter hardening operation after sintering can yield complex microstructures. In this study, the sinter hardened samples with varying copper content exhibited pearlite, martensite and bainite-like phases in their microstructure. Steels containing carbide forming elements like Cr and Mo can also alter the classical lamellar structure of pearlite. To understand the complex microstructures of sinter hardened samples more clearly, a normalizing heat treatment was applied to several sintered specimens.

4.3.1. Microstructural Development in Normalized Samples

As an initial step, copper free and 2% Cu containing samples were normalized to examine the present phases in the microstructures. The sinter hardened specimens were austenitized at 850^{o}C for 10 minutes and then, cooled in air.

Figure 18 and 19 exhibits the microstructure of normalized samples having 0% Cu and 2% Cu respectively. The dark regions in the micrographs appear to be pearlitic whereas the brighter colored islands with a yellow tint are most probably martensite. The amount of martensite in the samples with 2% Cu seems to be higher when Figures 20 and 21 are compared. Though few, at definite regions small red copper powder particles are also seen indicating that they did not dissolved in the matrix totally after sintering (Figure 19).

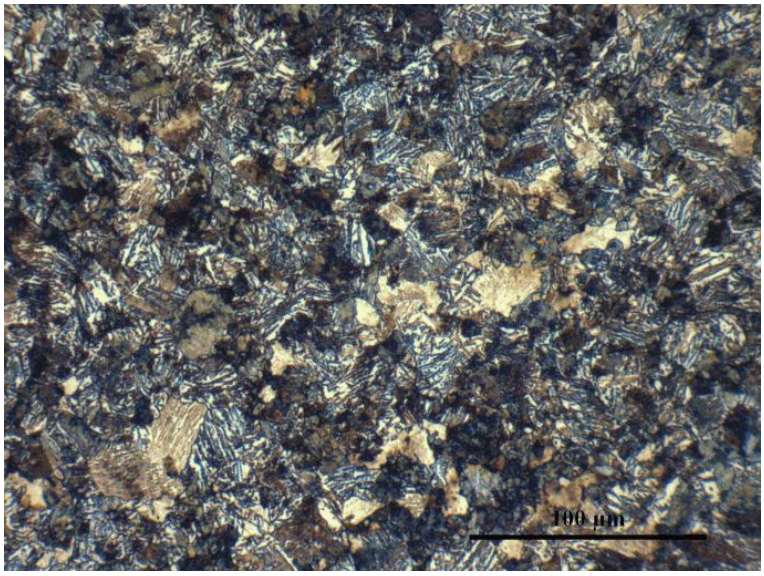

Figure 18: Optical micrograph of Astaloy 85 Mo with 0.8% graphite after normalization heat treatment.

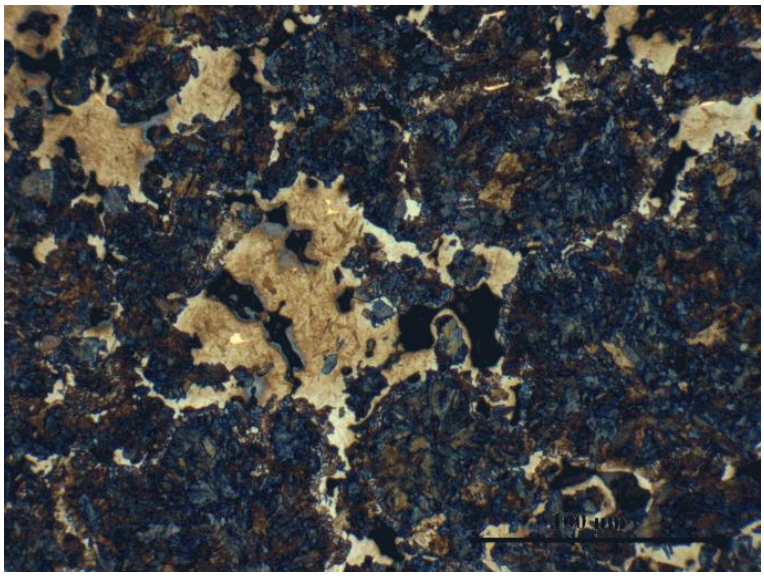

Figure 19: Optical micrograph of Astaloy 85 Mo with 0.8% graphite and 2% copper after normalization heat treatment.

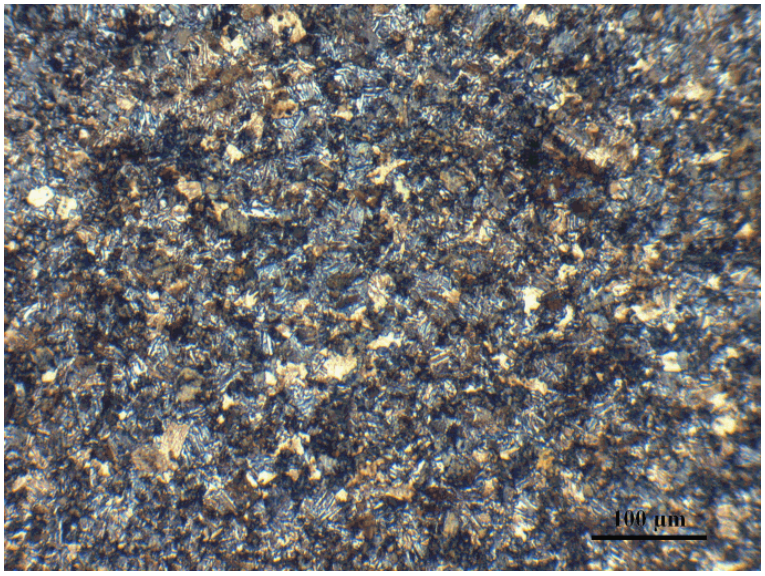

Figure 20: Optical micrograph of Astaloy 85 Mo with 0.8% graphite after normalization heat treatment.

In specimen having 2% Cu, it is observed that the martensitic transformation took place preferentially at the particle boundaries at definite regions (Figure 21). However, isolated martensite islands could also be seen within the same specimen.

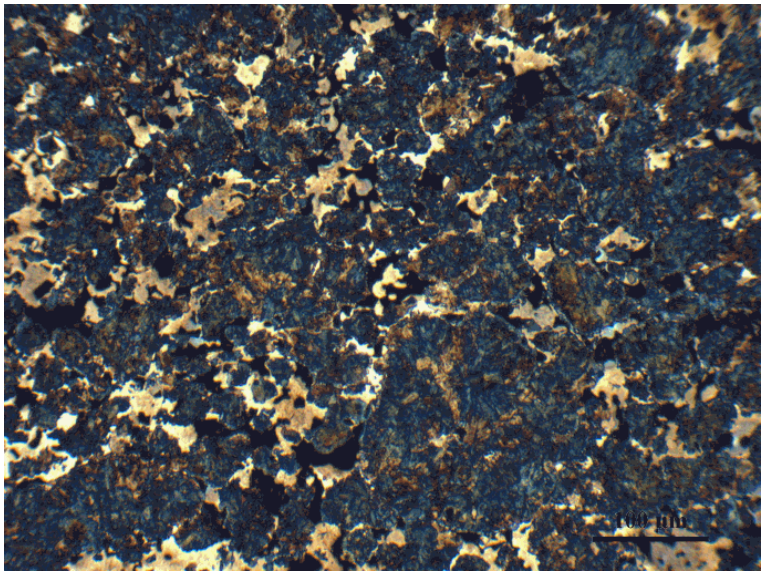

Figure 21: Optical micrograph of Astaloy 85 Mo with 0.8% graphite and 2% copper after normalization heat treatment.

Some dark regions are also detected within the microstructure which has a different morphology than pearlite under optical microscope. In order to observe the morphology of the phases present in the normalized samples in more detail, SEM is used.

The pearlite morphology is seen more clearly under SEM (Figure 22). At a higher magnification it is seen that the pearlite morphology in the samples are different than the classical lamellar morphology (Figure 23). At definite regions the cementite has an acicular structure. However, in other regions classical lamellar structure can be observed as well. This can be attributed to the presence of Mo in the steel, which probably modifies the pearlitic structure and it causes the formation of acicular ferrite with carbide.

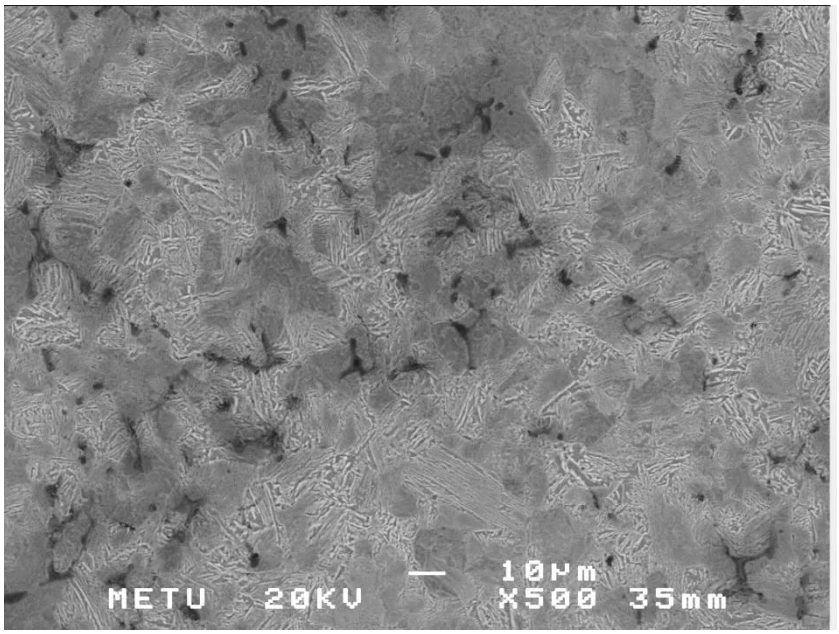

Figure 22: SEM micrograph of Astaloy 85 Mo with 0.8% graphite after normalization heat treatment.

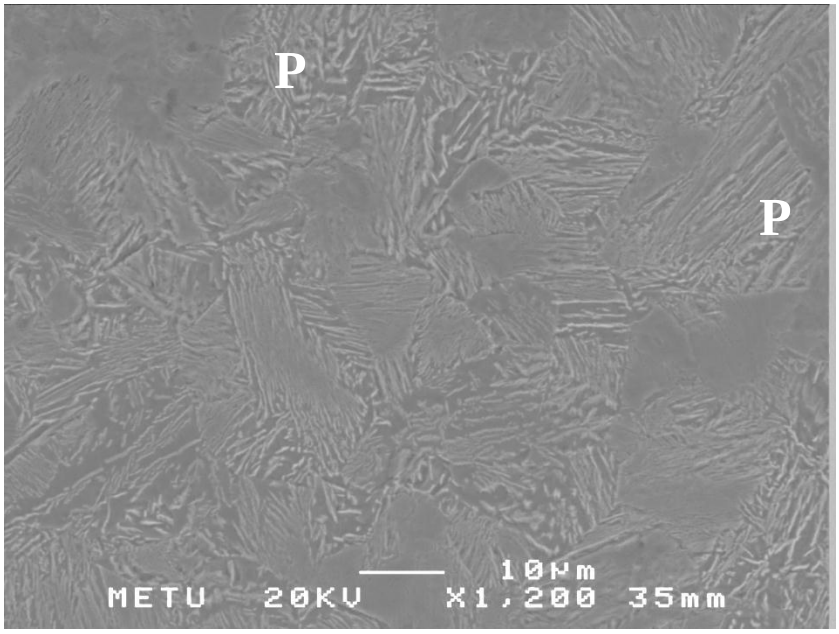

Figure 23:SEM micrograph of Astaloy 85 Mo with 0.8% graphite after normalization heat treatment. Pearlite phase is shown as “P”.

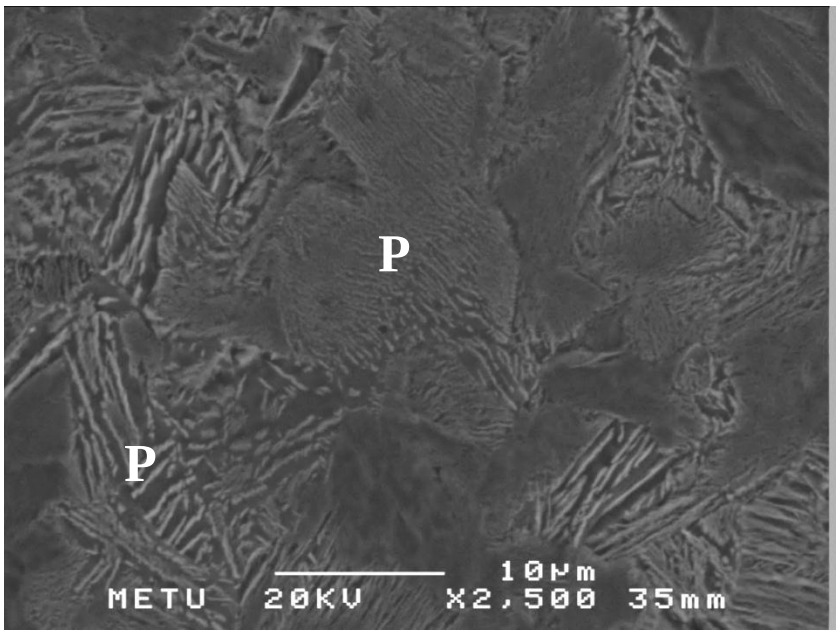

Figure 24:SEM micrograph of Astaloy 85 Mo with 0.8% graphite after normalization heat treatment. Pearlite phase is shown as “P”.

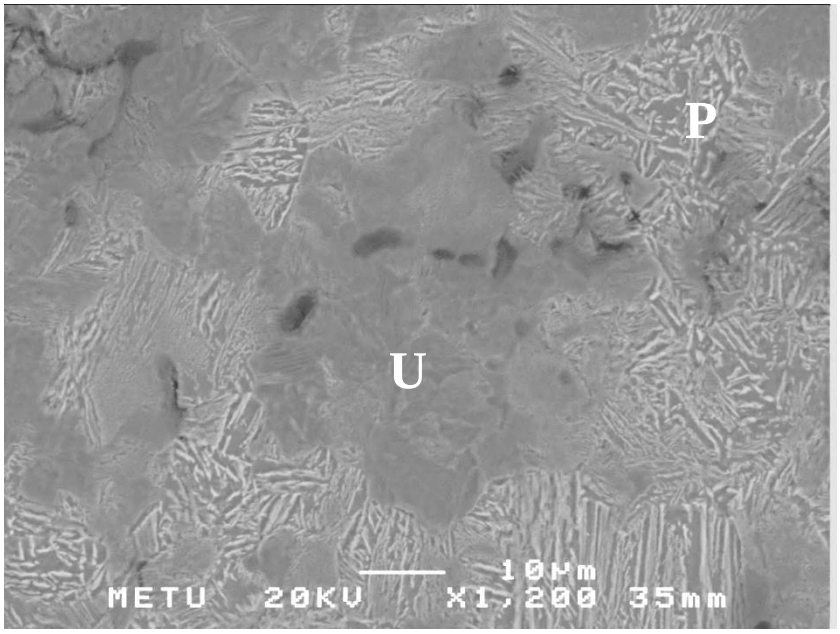

Figure 25: SEM micrograph of Astaloy 85 Mo with 0.8% graphite after normalization heat treatment. The pearlite phase is shown with “P” whereas the unknown phase is marked as “U”.

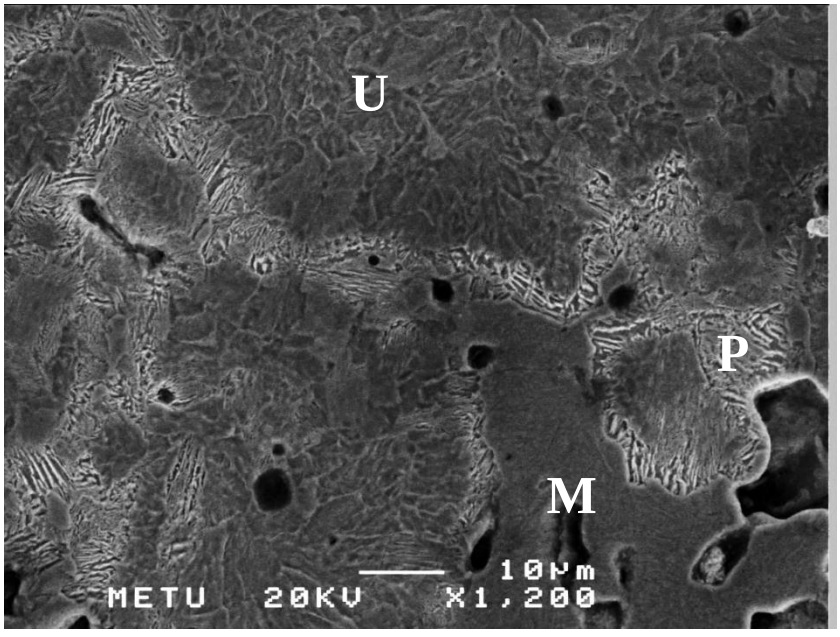

Figure 26:SEM micrograph of Astaloy 85 Mo with 0.8% graphite and 2% Cu after normalization heat treatment. The pearlite phase is shown with “P” and martensite phase is marked as “M” whereas the unknown phase is shown with “U”.

More important, there are several phase islands with a different morphology. One of these regions is shown in Figure 25 and 26. The pearlite phase is shown as "P" in Figure 25 and 26. The unknown phase mixture, which is shown as "U" on the same micrographs does not have either a lamellar or an acicular structure. In order to define this phase mixture, microhardness indentations were taken. Figure 27 shows an indentation taken from that undefined region. The microhardness values of this unknown phase are in the range 350 – 400 HV which indicates that this region is not a pearlite phase. To make a correlation between microhardness values, several indentations were also taken from martensitic regions as seen in Figure 28. The microhardness value of this indentation is 925 HV0.1 (77 HRC) and indicates that the light coloured islands are martensite.

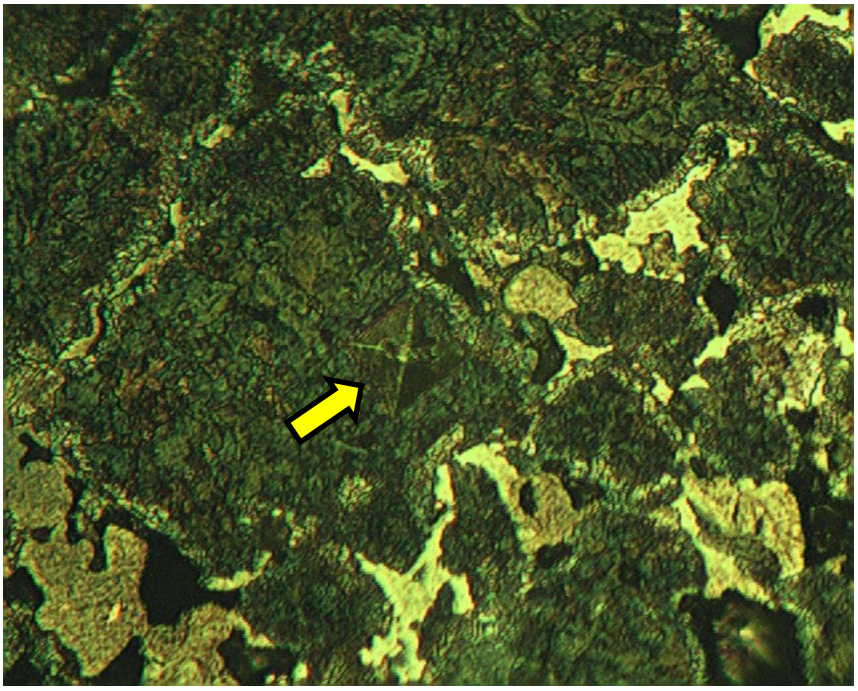

Figure 27: A microhardness indentation taken from bainitic region.

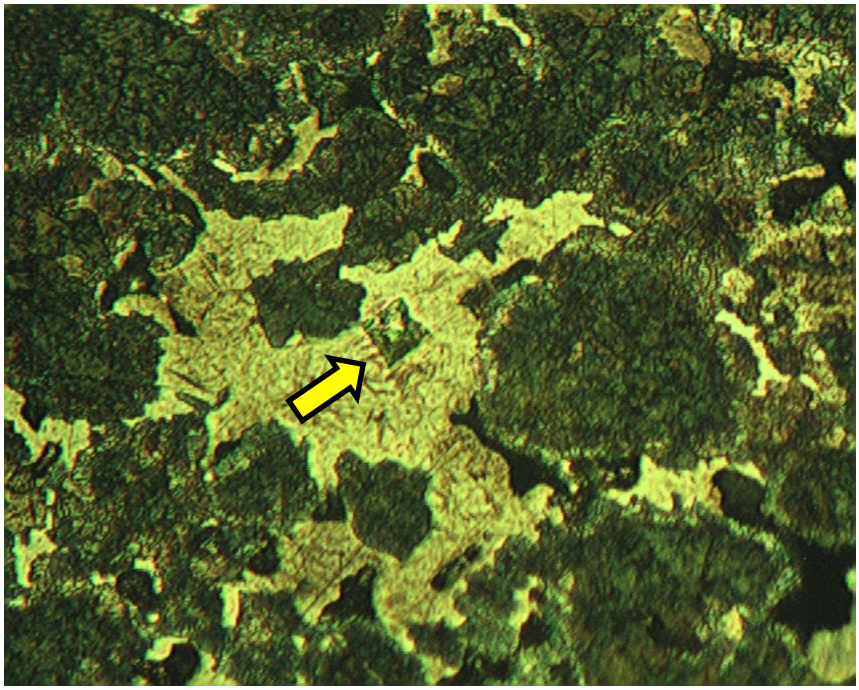

Figure 28: A microhardness indentation taken from martensitic region.

4.3.2. Microstructural Development of Sinter Hardened Specimens

After identification of the phases present in normalized samples, the microstructural characterization of sinter hardened samples was done. In the all sinter hardened specimens, depending on the composition and cooling rate, pearlite, bainite, and/or martensite were obtained. The details of the morphology of the phases are discussed by using optical and SEM micrographs.

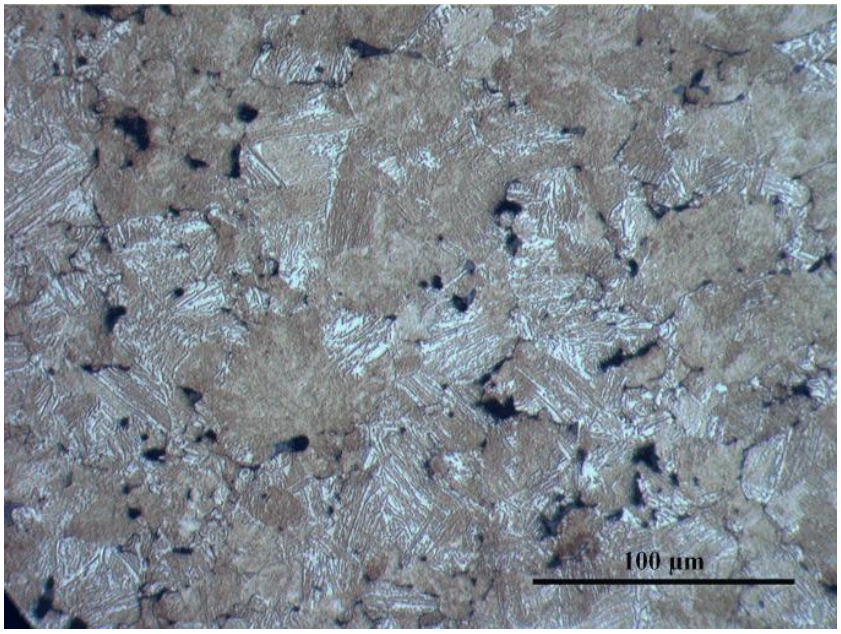

Figure 29: Optical micrograph of Astaloy 85 Mo with 0.8% graphite after cooling at a rate of 0.5^{0}C/sec.

The samples consisting of Astaloy 85 Mo with admixed 0.8% C have nearly fully pearlitic microstructures and very similar to that of normalized copper free samples. As can be seen in Figure 29, 30, and 31, the change in cooling rate does not have a significant effect on the microstructure. The brighter phase in the micrographs is coarse pearlite and the darker one is most probably bainite and fine pearlite. As can be seen in Figure 29, 30 and 31, lamellar spacing of fine pearlite is too narrow and it is even difficult to resolve under optical microscope. Additionally, the dark regions seen in Figure 29, 30 and 31 also contain unknown phase mixture which was previously observed in normalized samples.

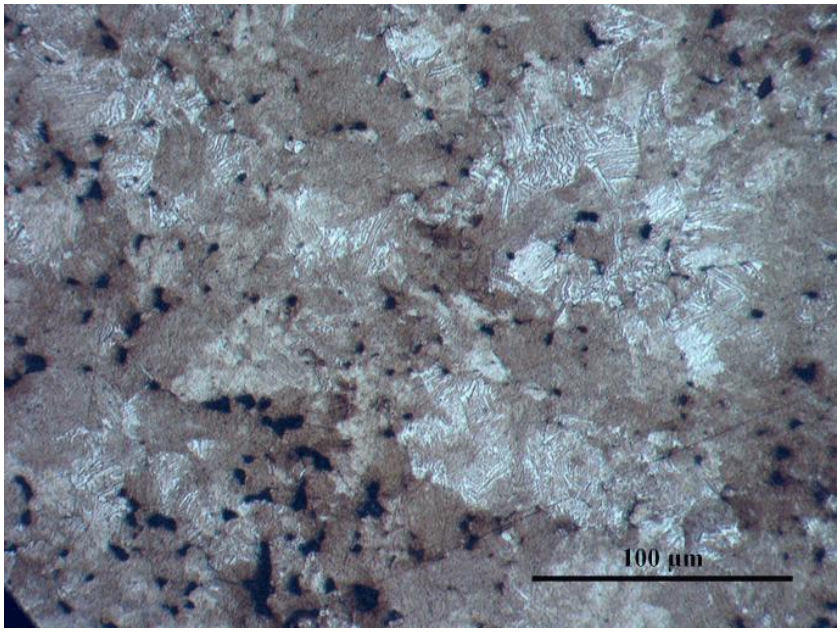

Figure 30: Optical micrograph of Astaloy 85 Mo with 0.8% graphite after cooling at a rate of 1.5^0C/sec.

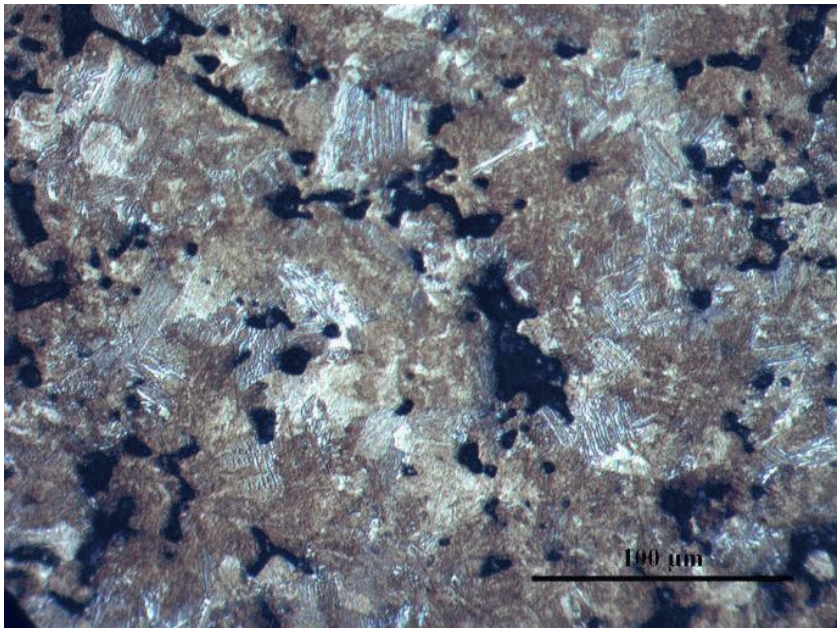

Figure 31: Optical micrograph of Astaloy 85 Mo with 0.8% graphite after cooling at a rate of 3^0C/sec.

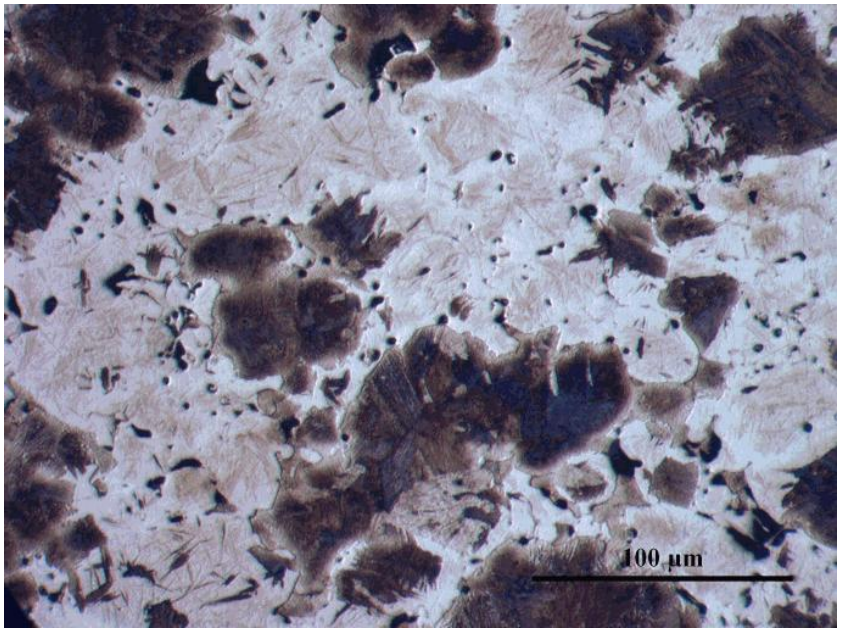

Figure 32: Optical micrograph of Astaloy 85 Mo with 0.8% graphite and 1% Cu after cooling at a rate of 0.5^0C/sec.

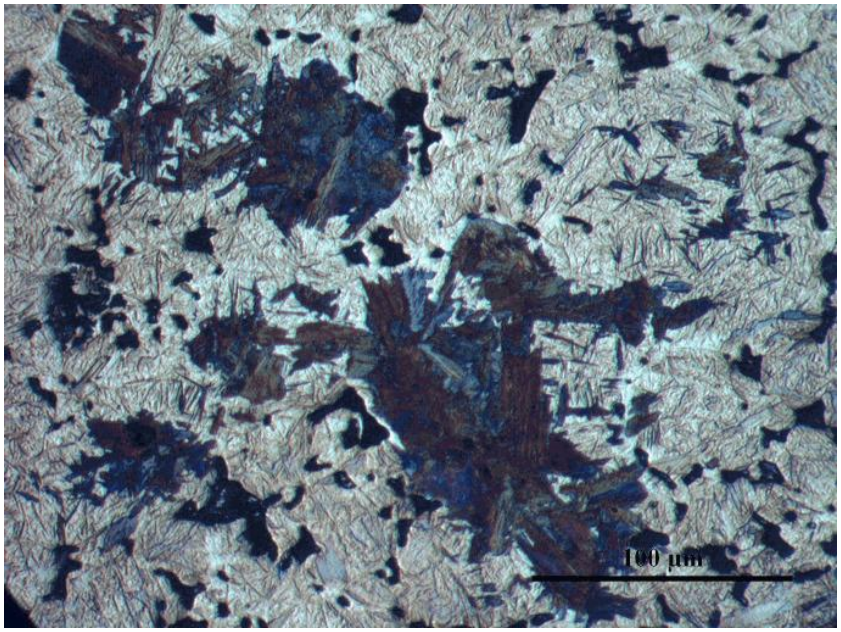

Figure 33: Optical micrograph of Astaloy 85 Mo with 0.8% graphite and 1% Cu after cooling at a rate of 1.5^0C/sec.

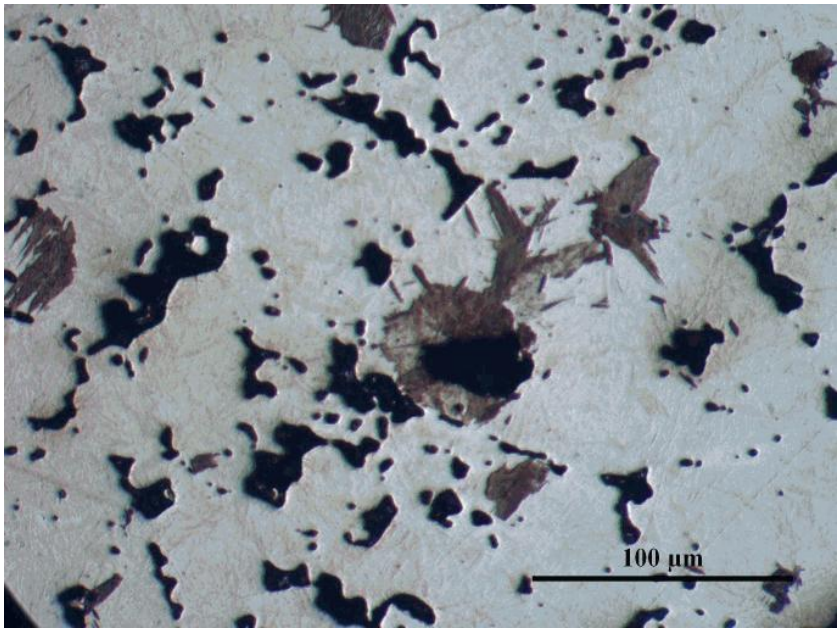

Figure 34: Optical micrograph of Astaloy 85 Mo with 0.8% graphite and 1% Cu after cooling at a rate of 3^0C/sec.

When Figure 29, 30 and 31 are compared with respect to the increase in cooling rate, the only noticeable effect is the presence of a few islands of martensite at higher cooling rates.

However, addition of 1% Cu enhanced the martensite formation. Figure 32 belongs to Astaloy 85 Mo with 0.8% graphite and 1% Cu. When Figure 29 and 32 are compared, it can be seen that content of the dark phase (presumably pearlite and bainite phase mixture) decreases considerably which can be attributed to the effect of copper. The light contrasted matrix phase in Figure 32 is martensite phase. Martensite content increases with an increase in cooling rate in the samples containing 0.8% C and 1% Cu (Figure 32, 33, and 34).

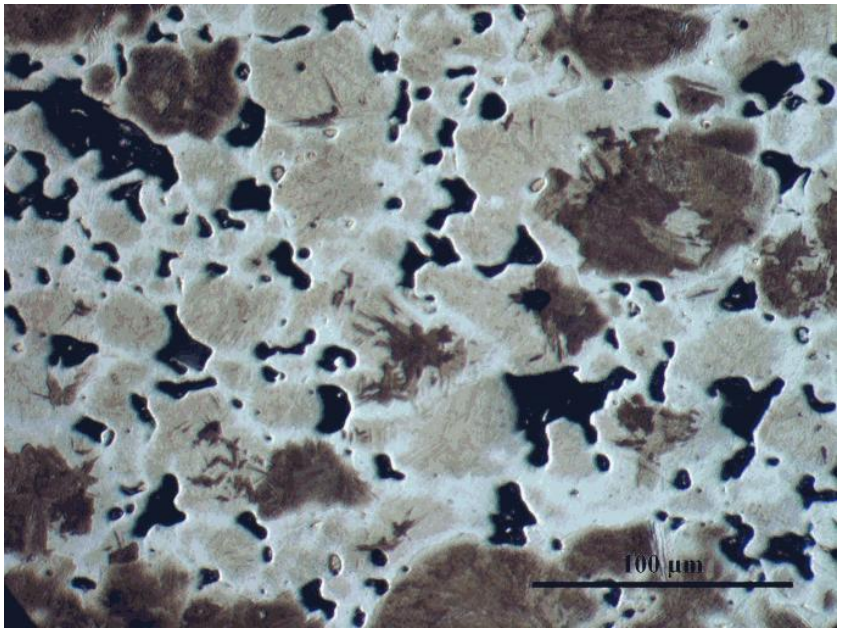

Figure 35: Optical micrograph of Astaloy 85 Mo with 0.8% graphite and 2% Cu after cooling at a rate of 0.5^0C/sec.

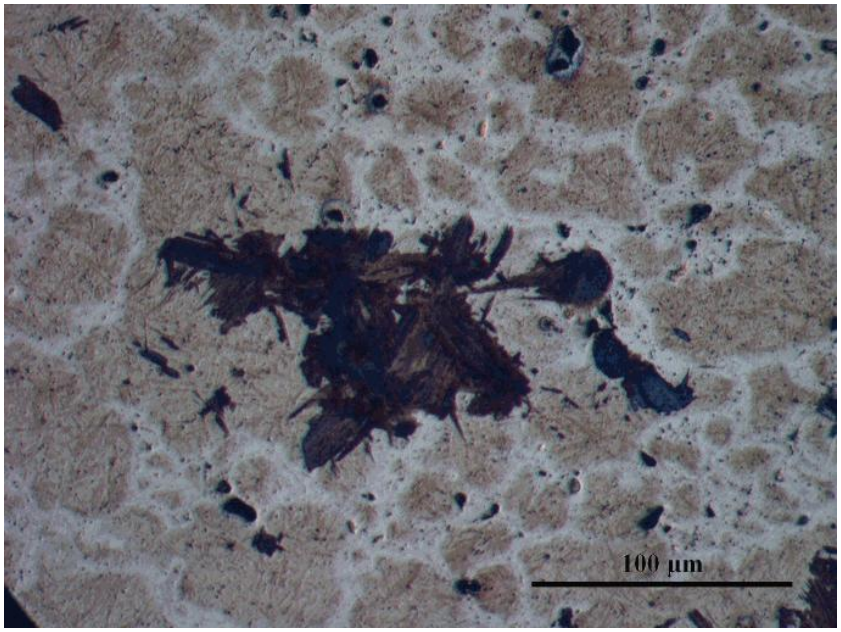

Figure 36: Optical micrograph of Astaloy 85 Mo with 0.8% graphite and 2% Cu after cooling at a rate of 1.5^0C/sec.

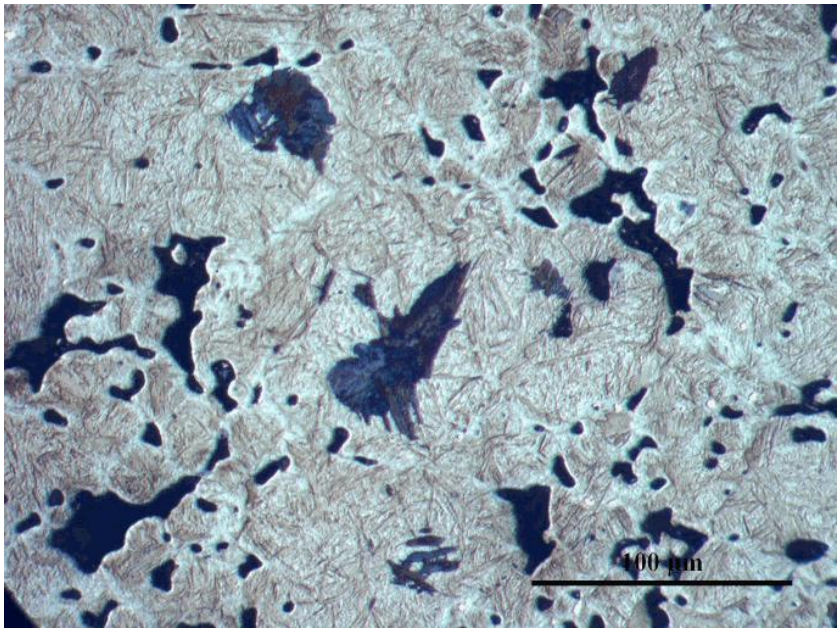

Figure 37: Optical micrograph of Astaloy 85 Mo with 0.8% graphite and 2% Cu after cooling at a rate of 3^0C/sec.

Astaloy 85 Mo admixed with 0.8% C and 2% Cu sample has similar microstructural constituents when compared to the samples having 1%Cu after cooling at a rate of 0.5^oC/sec (Figure 35) The dark phase content decreases but the amount of martensite phase increases when the copper content in the samples increased from 1% Cu to 2% Cu. For 2% Cu, the matrix phase is martensite and there are only a few pearlitic-bainitic islands (dark phase) as can be seen in Figure 35, 36 and 37. In order to examine the detailed morphology of the phases, SEM studies were done.

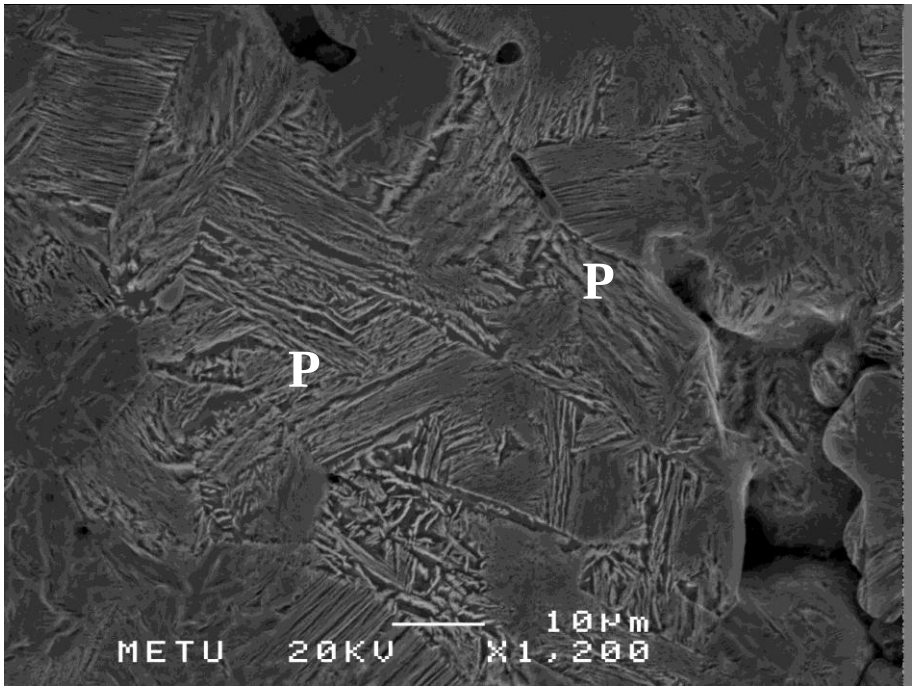

Figure 38: SEM micrograph of Astaloy 85 Mo with 0.8% graphite after cooling at a rate of 0.5^{o}C/sec. The micrograph shows the morphology of pearlite (“P”)

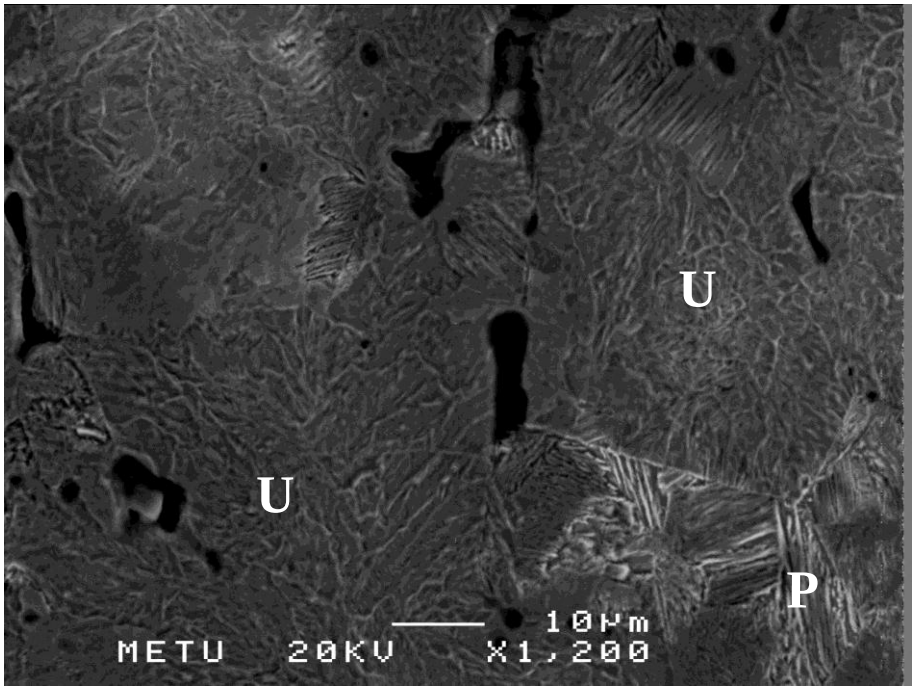

Figure 39: SEM micrograph of Astaloy 85 Mo with 0.8% graphite after cooling at a rate of 1.5^{o}C/sec. The unknown phase is marked as "U".

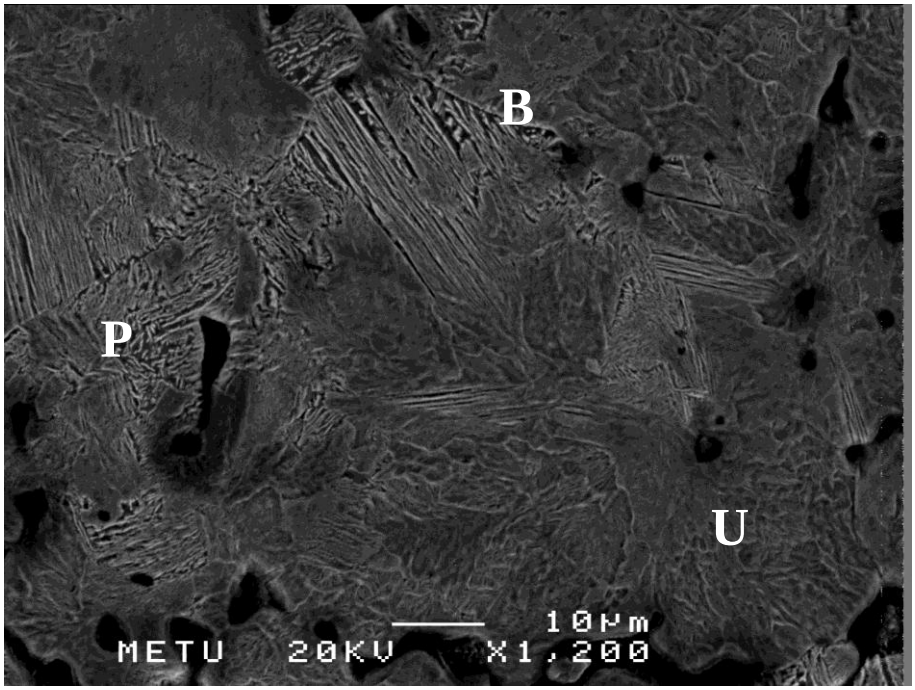

Figure 40: SEM micrograph of Astaloy 85 Mo with 0.8% graphite after cooling at a rate of 3^{o}C/sec. In this specimen, the fine acicular phase is most probably lower bainite (“B”).

As shown in Figure 38-40, the microstructure of the samples with no copper is mainly pearlitic. A few lower bainite phase is also detected, especially in fast cooled specimens (shown as "B" in Figure 40). The pearlite at definite regions has a very fine lamellar morphology. The unknown phase mixture, which was previously observed in normalized specimens is also seen in sinter hardened specimens (shown as “U” in Figure 40). The morphology and the microhardness values of the unknown phase “U” is very similar to that of normalized samples (350-400 HV(0.1)). This hardness range together with the non-acicular morphology, the unknown regions can be either upper bainite or globular bainite.

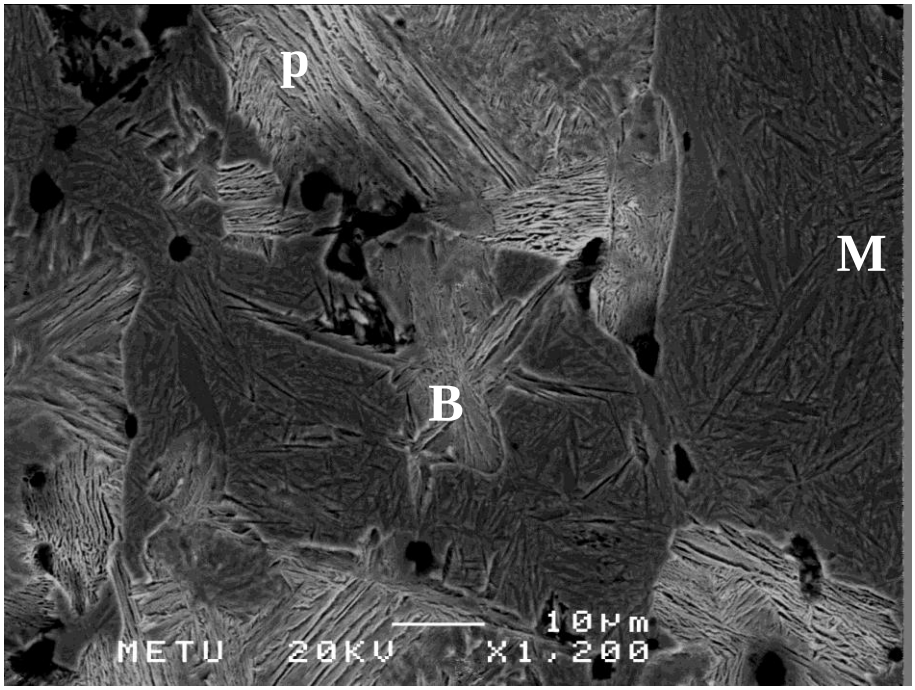

Figure 41: SEM micrograph of Astaloy 85 Mo with 0.8% graphite and 1% Cu after cooling at a rate of 0.5°C/sec.

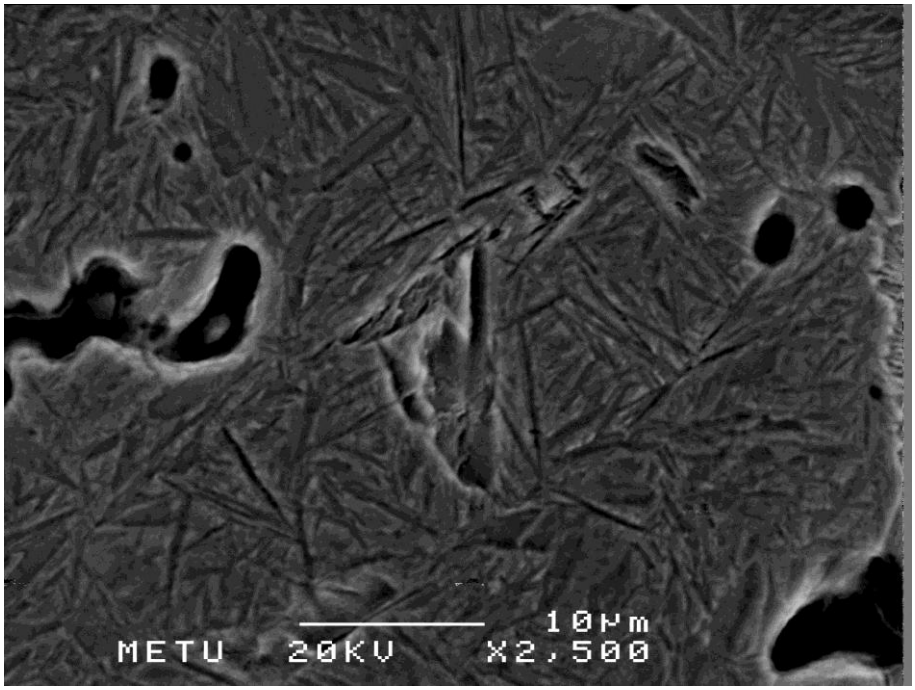

Figure 42: SEM micrograph of Astaloy 85 Mo with 0.8% graphite and 1% Cu after cooling at a rate of 0.5°C/sec.

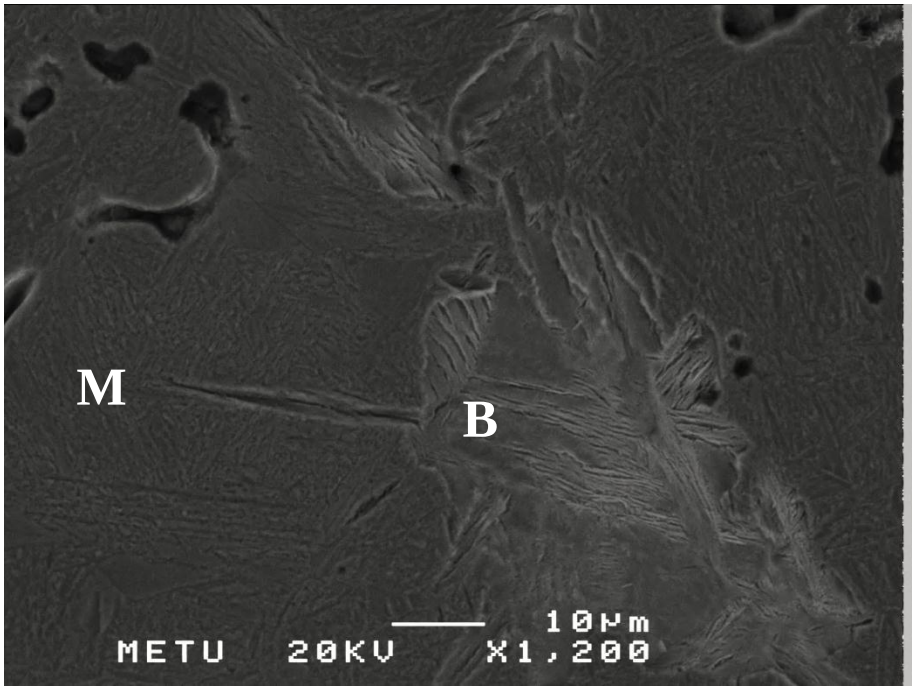

Figure 43: SEM micrograph of Astaloy 85 Mo with 0.8% graphite and 1% Cu after cooling at a rate of 3^{o}C/sec.

As seen in Figure 41, Astaloy 85 Mo having 1% Cu exhibits pearlite - lower bainite and martensite phases together after cooling at a rate of 0.5^{0}C/sec. The dark contrasted areas with an acicular morphology in the microstructure are mainly martensite phase. Martensite phase is seen at a higher magnification in Figure 42. In Figure 43, lower bainite and martensite can be seen together in 1%Cu specimen after cooling at a rate of 3^{o}C/sec.

In view of these observations it can be stated that the dark phase seen in optical micrographs belongs to bainite-pearlite phase mixtures in fast cooled specimens. As expected, both Cu and the cooling rate increases the martensite and lower bainite content.

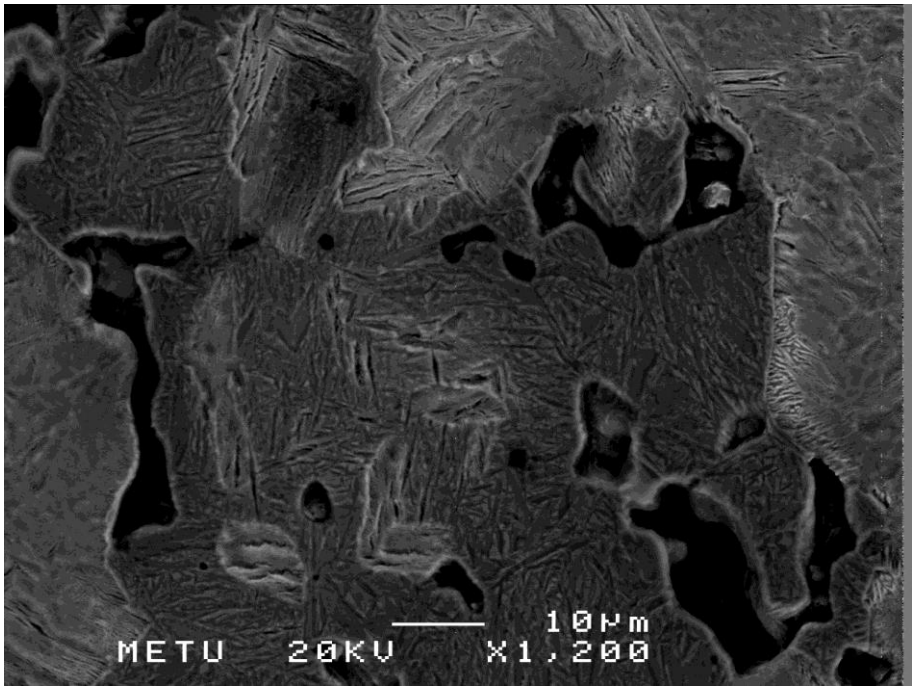

Figure 44: SEM micrograph of Astaloy 85 Mo with 0.8% graphite and 2% Cu after cooling at a rate of 0.5^{o}C/sec.

Astaloy 85 Mo admixed with 0.8% C and 2% Cu sample has a similar microstructural morphology with the samples having 1% Cu after cooling at a rate of 0.5^{o}C/sec. as seen in Figure 44. Figure 44 reveals that martensitic matrıx has also some lower bainitic regions. As the post sintering cooling rate increases from 0.5^{o}C/sec to 3^{o}C/sec, the microstructure becomes almost fully martensitic with a few lower bainite regions as seen in Figure 45.

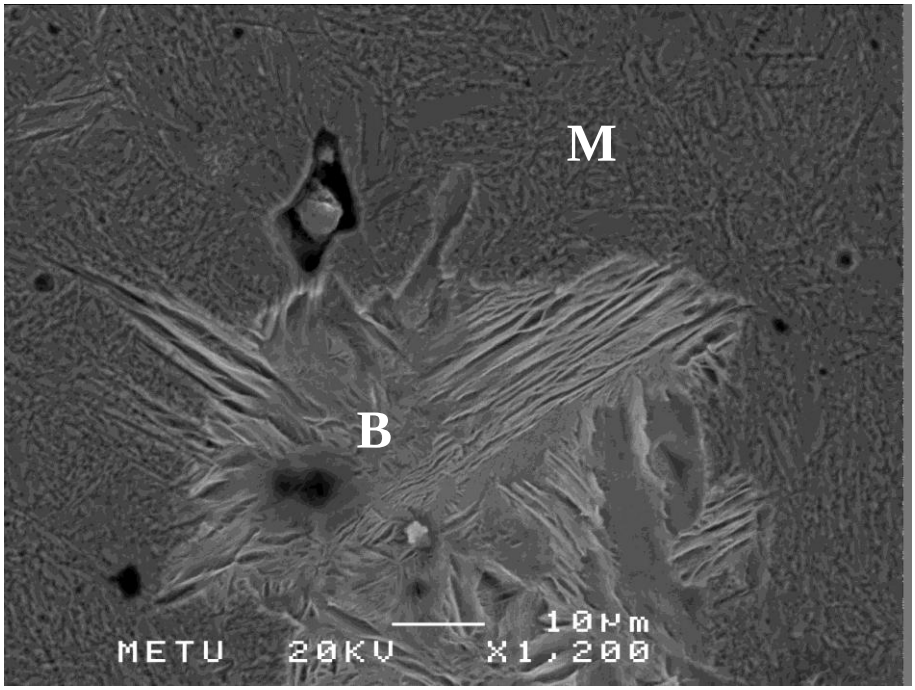

Figure 45: SEM micrograph of Astaloy 85 Mo with 0.8% graphite and 2% Cu after cooling at a rate of 3^{o}C/sec.

The results from characterization by optical microscopy and SEM are also verified by the results of microhardness measurements. Microhardness measurement was used for characterizing the phases in this study. Martensitic, bainitic and pearlitic areas within microstructure were investigated with microhardness measurements. In addition, bainite in the microstructures is present as pearlite-bainite and/or martensite-bainite phases mixtures. For this reason, it was difficult to measure hardness of an isolated bainite region. The hardness of the dark, unknown phase observed in specimens is also included into Table 3.

Table 3: Microhardness values of pearlite, bainite, martensite and dark phase in sinter hardened Astaloy 85 Mo admixed with 0.8% C and varying copper content (0% Cu – 1% Cu – 2% Cu) powder alloys

Microstructures	**Hardness Range (HV 0.1)**
Pearlite	280 – 385
Dark phase (marked as ”U”)	350-400
Bainite – pearlite phase mixture	435 – 625
Martensite	745 – 1070

It is difficult to measure microhardness values from isolated bainite region because needle like lower bainite is present as bainite – pearlite and/or martensite – bainite phases mixtures. Also, bainite – pearlite phase mixture has not only lower bainite but also contains the dark phase which is most probably upper bainite or globular bainite. Microhardness of martensite and bainite has a wide range due to this reason (Table 3).

4.3.3. The Behaviour of Copper in Sinter Hardened Samples

In samples containing 1% Cu or 2% Cu, the distribution of the phases are not homogeneous. As seen in Figure 46 at definite locations, the martensite phase prefers the powder boundaries. Also seen in Figure 35 and 36, the etching behaviour of martensite phase at the powder boundaries and within the powder is different. It is difficult to determine the original austenite boundaries and powder boundaries in sintered specimens. Nevertheless, the inhomogeneous phase distribution can be resolved.

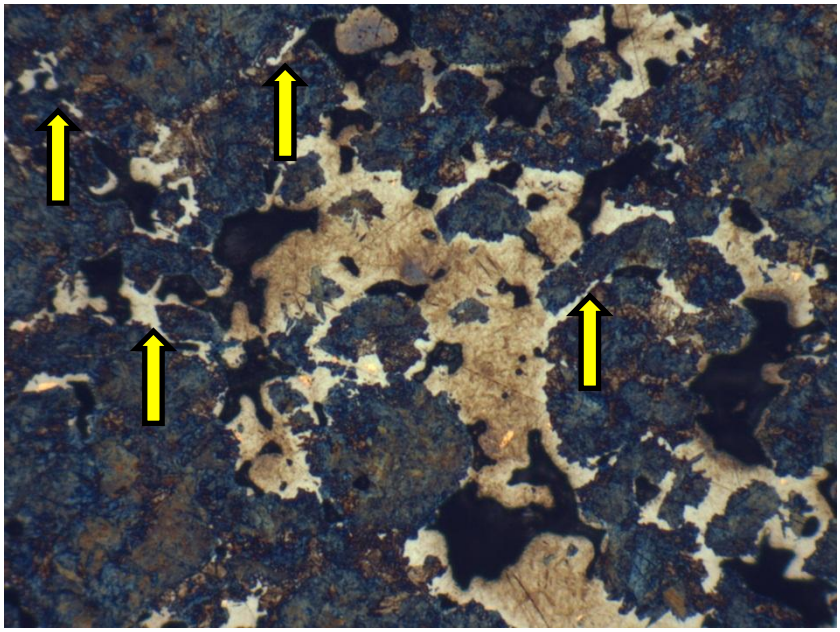

Figure 46: Optical micrograph of Astaloy 85 Mo with 0.8% graphite and 2% copper after normalization heat treatment.

It is a well-known fact that in sintered specimens Cu forms a liquid phase and spreads around the powder boundaries. As a result, the sintered densities are improved. It is possible that Cu behaves similar in sinter hardened specimens such that powder boundaries contain higher amount of Cu in solid solution. In order to find the distribution of Cu in the matrix X-ray mapping was done.

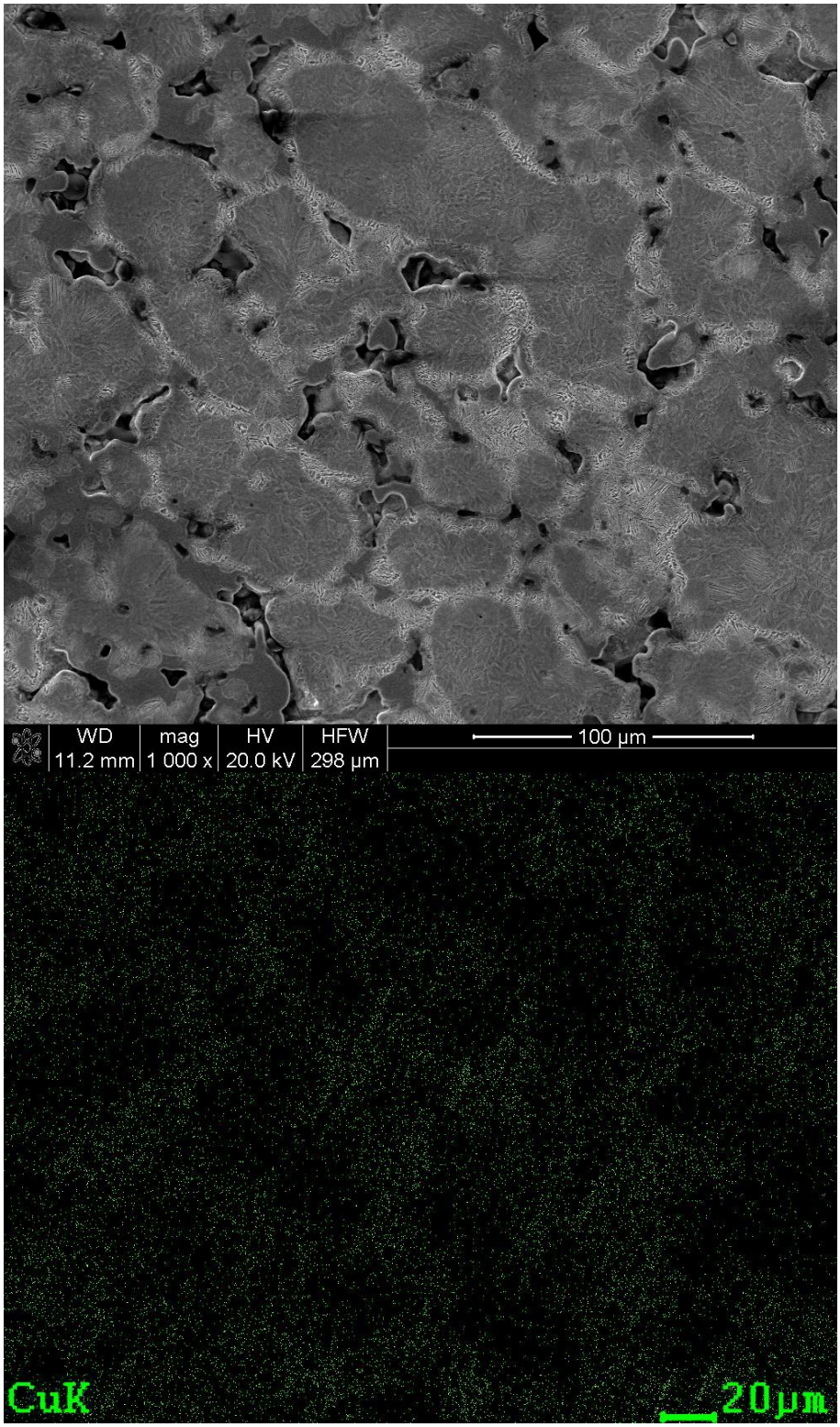

Figure 47: The SEM micrograph of the specimen having 2% Cu and the X-ray mapping of Cu within the same region.

In view of these results, it can be stated that powder boundaries have slightly higher amount of Cu.

4.4. Pearlite Content of the Samples

The pearlite content in steels can be differentiated with different methods. In this thesis study, selective etching by 2% Nital etchant is applied to determine the volume fraction of pearlite in the samples. Etching rate of the phases is critical for selective etching. Pearlite develops at an earlier stage with respect to bainite and martensite. With longer etching times, bainite can be observed before martensite phase. Using selective etching, the pearlitic regions in the samples were developed and the volume fraction of the pearlite phase was calculated using image analyzer software. It is important to note that dark phase was also etched during selective etching. As can be seen in Figure 48, the pearlitic regions are shaded green. Figure 48 reveals that the amount of pearlite decreases with an increase in cooling rate and Cu content.

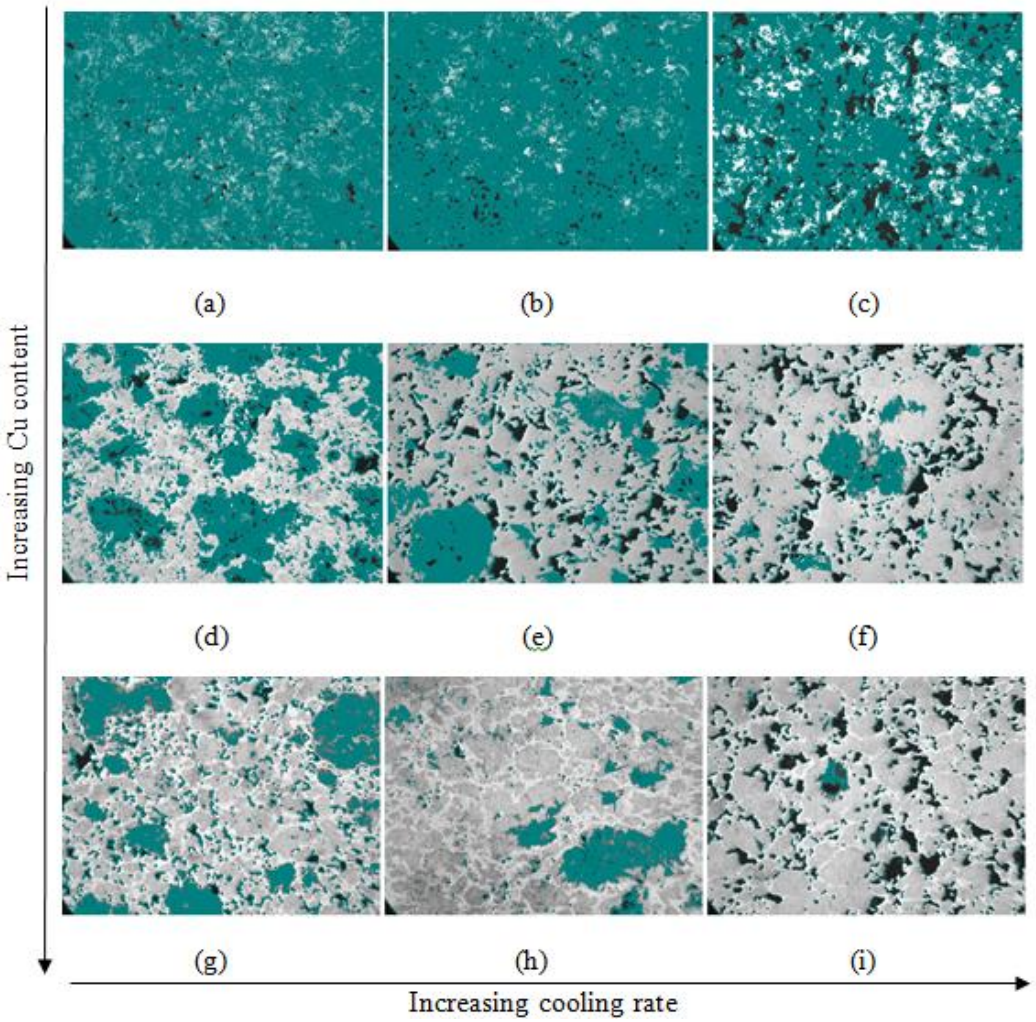

Figure 48:The change in pearlite content with Cu content and cooling rate.

The results of image analysis are plotted in Figure 49. As seen, addition of only 1% Cu increases the amount of martensite. With the addition of 1% Cu, the amount of martensite is increased from 0% to approximately 60% even after a relatively slow cooling rate of 0.5^{o}C/sec. Also, Figure 48 reveals that Astaloy 85 Mo with 0.8% C and 2% Cu with 3^{o}C/sec. post sintering cooling rate has almost fully martensitic structure.

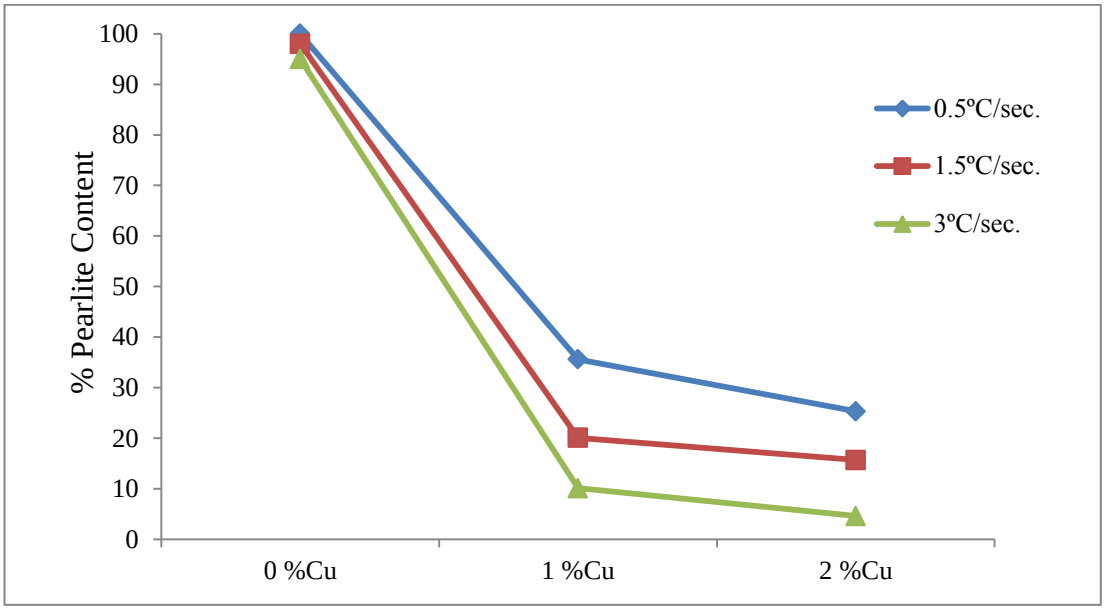

Figure 49: The change in the pearlite content with varying cooling rate and copper content

4.5. Macrohardness Measurements

Macrohardness tests are carried out for sinter hardened samples. As seen in Figure 50, the hardness of the samples increases proportionally with an increase in cooling rate and copper content. This increase is attributed to the increase in the amount of martensite. It must be noted that the 1% Cu and 2% Cu containing specimens yielded very similar hardness values at different cooling rates.

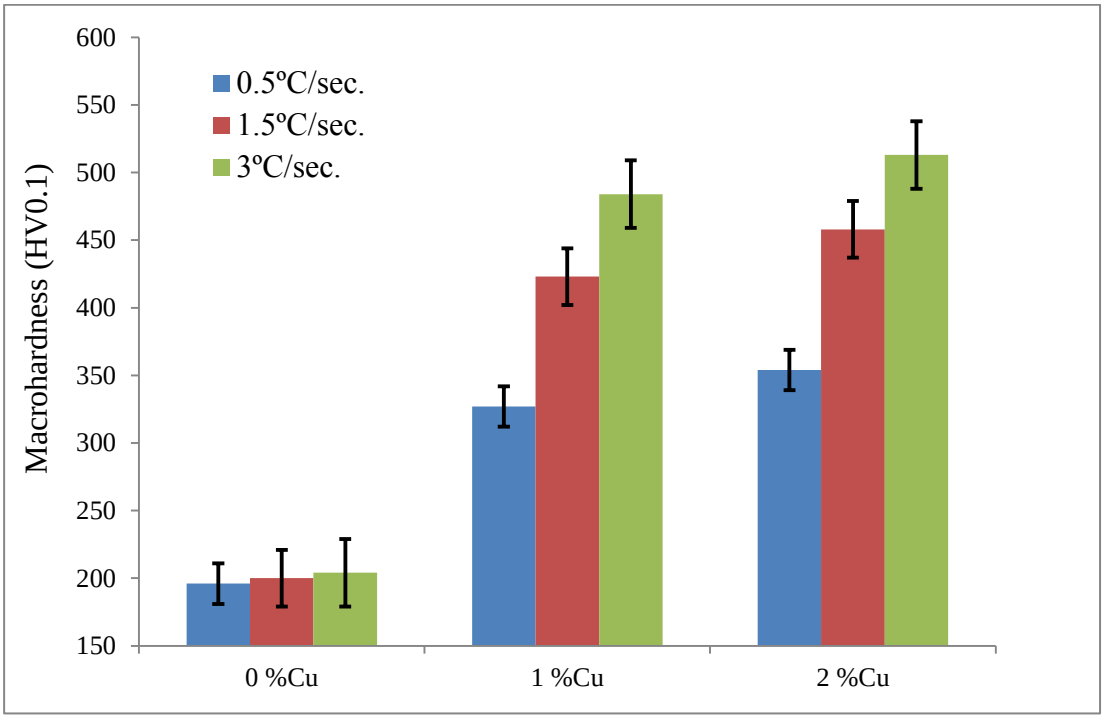

Figure 50: Macrohardness values of Astaloy 85 Mo with varying copper content.

4.6. Transverse Rupture Strength Test Results

Transverse rupture strength (TRS) tests were conducted with the samples which are sinter hardened. The samples having 1% Cu and 2% Cu yielded lower TRS values (Figure 51). Moreover, the Cu containing samples exhibited lower TRS with an increase in cooling rate. In the previous sections, it was shown that amount of martensite increases with increasing post sintering cooling rate and % Cu content.

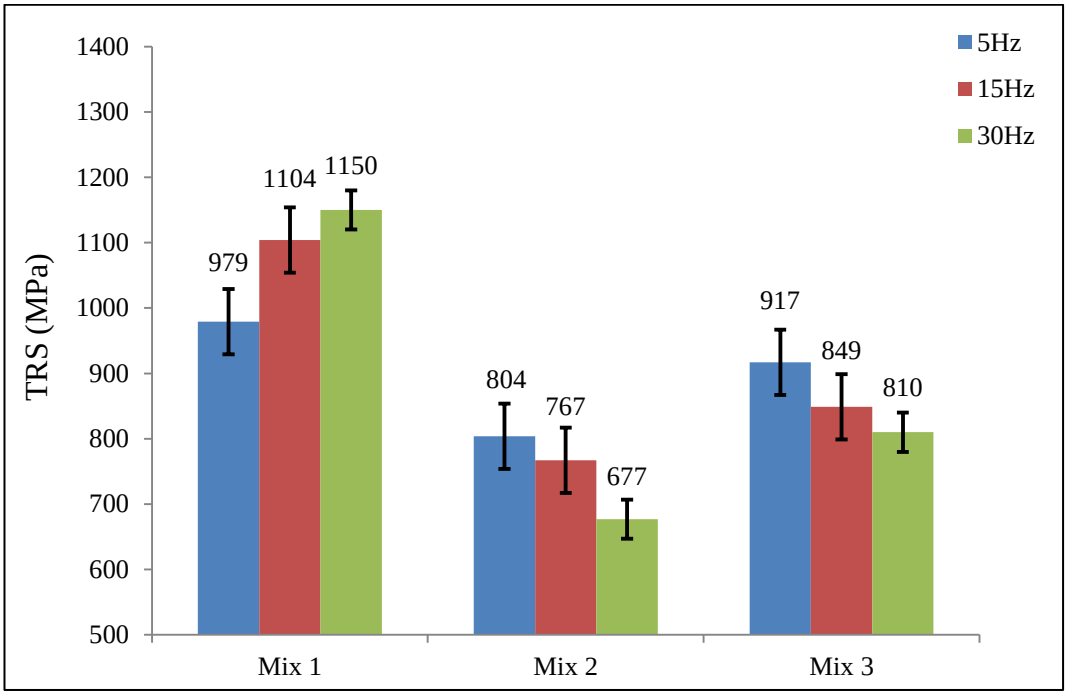

Figure 51: The change in TRS with varying cooling rate and copper content.

CHAPTER 5

DISCUSSION

In this thesis study, the effect of sinter hardening on mechanical properties of Astaloy 85 Mo (Fe-0.85Mo) powder admixed with 0.8% C and 0% Cu, 1% Cu and 2% Cu was investigated. Two important parameters, namely the effect of copper content and effect of post sintering cooling rate on microstructure and mechanical properties are studied.

Molybdenum is an important alloying element in powder metallurgy industry because it increases hardenability of the alloy, while its addition does not make critical changes on compressibility of the powder alloy when compared to other alloying elements [24]. The price of molybdenum increases significantly day to day due to the attraction in the industry. For this reason, powder metallurgy industry heads towards leaner molybdenum content alloys [25]. Until today, alloys contain 2% Mo or 1.5% Mo has been used for sinter hardening applications [17]. It is a well-known fact that Mo enhances the strength of the powder metallurgy alloys [20, 24, 29]. In this study, the addition of only 0.85% Mo enhanced the formation of martensite. However, as will be discussed in the following section (5.3), the transverse rupture strength values are not improved.

5.1. The Porosity Content of Sinter Hardened Samples

Effect of copper on porosity content of sintered samples was given in Table 2. As copper content increases from 0% to 2%, the amount of porosity decreases from 12.1% to 8.6%. Copper is liquid at sintering temperature (1120^{o}C) and most probably spreads over iron matrix during sintering. This is an expected result since the positive effect of copper in sintered densities is well documented [9, 13, 16, 17, 23, 27]. The sintering kinetics is slow at the common sintering temperatures which are 1120^{o}C-1150^{o}C and the diffusion of alloying elements is also limited at these temperatures. The acceleration of the atomic mass transport mechanisms can be provided with liquid phase sintering [17]. The melting point of copper is 1083^{o}C and copper spreads in the iron matrix via liquid phase sintering during sintering cycle. The beneficial effect of copper on mechanical properties, its low cost and availability in the powder form makes copper as a common alloying element in the powder metallurgy industry [27]. It is known that liquid copper migrates to porous regions and sharp edges and corners of particles and enables a decrease in porosity content by creating a more efficient packing of particles [13]. Presence of a liquid phase during sintering also enhances atomic mass transport mechanisms.

5.2. Microstructural Development of Sinter Hardened Specimens

Sinter hardening operation after sintering can yield complex microstructures. To understand the complex microstructures of sinter hardened samples more clearly, a normalizing heat treatment was also applied to several sintered specimens. All microstructural investigation is carried out in both sinter hardened and normalized samples. It must be noted that the microstructural development of the normalized microstructures were very similar to that of sinter hardened samples cooled at a rate of 0.5^{o}C/sec.

In all sinter hardened specimens, depending on the composition and cooling rate, pearlite, bainite-like phases and/or martensite were obtained.

The samples consisting of Astaloy 85 Mo with admixed 0.8% C have nearly fully pearlitic microstructures after sinter hardening. A molybdenum content of 0.85% alone was not enough for full hardenability of the sintered samples within these dimensions. Even after cooling at a rate of 3^{o}C/sec, only a few martensite islands were seen in samples without any Cu. As far as the pearlite is concerned, it is seen that the morphology of pearlite is different than the classical lamellar morphology (Figure 23). At definite regions the cementite has an acicular structure. However, in other regions classical lamellar structure can be observed as well. This is attributed to the presence of Mo in the steel, which probably modifies the pearlitic structure and it causes the formation of acicular ferrite with carbide. According to the study of Lindsley and Rutz, addition of molybdenum to powder alloys modifies the ferrite – carbide microstructure such that lamellar structure disappears and acicular ferrite with carbide and/or upper bainite appears [24]. Also, Mazancova et. al. revealed in their study that bainite is formed with same transformation mechanisms in the same temperature range with acicular ferrite [30]. Presence of molybdenum seems to enhance the formation of degenerated pearlite structure with acicular ferrite and carbide.

An increase in copper content and cooling rate has a critical effect on microstructural properties of Astaloy 85 Mo powder mixtures. In the samples containing 1% Cu or 2% Cu, nearly fully martensitic microstructures are attained after a cooling rate of 3^{o}C/sec (Figure 46 and 47). In view of these results it can be stated that Cu increases the hardenability by shifting TTT diagram to the right. Figure 9 is redrawn in Figure 51 to compare the effect of Mo and Cu. As seen, the effect of Cu on hardenability is not as strong as Mo. However, it seems that Cu together with Mo enables formation of nearly 100% martensite in sinter hardened samples at these dimensions.

An important finding in this study is the presence of a phase having a different morphology with respect to pearlite and bainite. As shown in Figures 26, 39 and 40, an unknown phase with a different morphology is detected. There is no acicular carbide precipitation or a lamellar structure indicating that the phase is not pearlite. On the other hand, it is also known that lower and upper bainite have acicular structures, which are quite different than this phase. Moreover, the microhardness values of this phase are found in the range 350 – 400 HV(0.1) which is higher than the pearlite regions.

In the literature, several phase transformation morphologies other than classical upper and lower bainite are also observed. These are named as globular bainite, inverse bainite, columnar bainite, pearlitic bainite and grain boundary lower bainite [31]. A comparison of the morphologies indicates that the unknown phase detected in this study can be globular bainite. The pesence of globular bainite is observed in several other studies [32-35]. It has been reported that the characteristic feature of globular bainite is the lack of carbides in the microstructure [31]. The evidences indicated that globular bainite is not different from ordinary bainite in its mechanism of transformation: The strange morphology is related to two factors: continuous transformation and low carbon content. In this thesis study, the continuous cooling of the samples upon sinter hardening or normalizing may possibly enhanced the formation of globular bainite. On the other hand, the samples contain 0.8% C which should avoid the formation of globular bainite. In view of these, it can be stated that the occurance of globular bainite needs further research, especially in powder metallurgy products.

As a concluding remark, all the phases detected in the specimens are summarized in Table 4. The transition from pearlite phase to martensite phase at different cooling rates and composition reflects the effect of Mo and Cu very well. The samples consisting of Astaloy 85 Mo with admixed 0.8% C have nearly fully pearlitic microstructures after sinter hardening. However, addition of Cu increases the amount of martensite, such that at fast cooling rates nearly 100% martensite is obtained.

Table 4: Microstructural features of sinter hardened Astaloy 85 Mo powder alloys with varying copper content. ("P" is pearlite, "GB" is globular bainite, "B" is bainite and "M" is martensite.)

Powder Mixture	**Cooling Rate (^{0}C/sec)**	**Obtained Phases**
Astaloy 85 Mo – 0.8% C	0.5	"P" with some "GB"
	1.5	"P" with some "GB"
	3	"P" with some "GB"
Astaloy 85 Mo – 0.8% C – 1% Cu	0.5	A mixture of "P", "B" and "M"
	1.5	A mixture of "P", "B" and "M"
	3	Nearly fully "M" with a few "P" and "B"
Astaloy 85 Mo – 0.8% C – 2% Cu	0.5	A mixture of "P", "B" and "M"
	1.5	A mixture of "P", "B" and "M"
	3	Nearly fully "M"

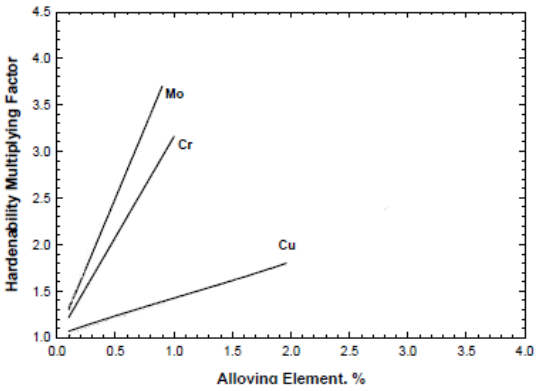

Figure 52: Effect of some alloying elements in hardenability. [23]

5.3. Mechanical Characterization of Sinter Hardened Samples

As shown in Figure 49, the hardness values of the samples are in the range 196-513 HV. As expected, an increase in the amount of martensite causes an incease in hardness values. As far as the transverse rupture strength tests are concerned, strength increases with an increase in cooling rate of copper free samples. On the other hand, TRS values decrease with an increase in cooling rate in the samples that contain copper. As mentioned above, Mo enhances the strength of the powder metallurgy alloys [20, 24, 29]. An increase in Mo content increases hardenability and hence the amount of martensite phase increases. Therefore, the increase in strength of the samples is attributed to the high amount of martensite. However, in this study an increase in the percentage of martensite caused a decrease in TRS values (Figure 50). A possible reason for this can be the extremely brittle nature of the martensite in as-quenched condition because no tempering operation is applied after sinter hardening. Moreover, the matrix contains residual pores which might also act as stress concentration points and can lower the TRS values. According to the study of Neilan et. al., brittle nature of martensite results in premature fracture in samples that contain high level of carbon [36]. Also in several other studies, it is found that the presence of untempered martensite may decrease the strength of the specimens [37, 38].

CHAPTER 6

CONCLUSIONS

Throughout this thesis study, the effect of sinter hardening on the mechanical and microstructural behavior of prealloyed Astaloy 85 Mo (Fe-0.85% Mo) powder with addition of 0.8% C and varying content of copper (1% Cu and 2% Cu) was examined. The powder alloys were sintered at 1120^{o}C for 20 minutes in an industrial sintering furnace and sinter hardened with post sintering cooling rates of 0.5^{o}C/sec., 1.5^{o}C/sec. and 3^{o}C/sec. in the same sintering cycle. The following conclusions can be drawn from the studies:

1- The amount of porosity of the samples were decreased with an increase in the copper content, which is attributed to the beneficial effect of copper on sintering.
2- The sinter hardened samples consisting of Astaloy 85 Mo with admixed 0.8% C have nearly fully pearlitic microstructures at all cooling rates. No martensite phase was detected.
3- The addition of copper did not only increase the attained densities but also impoved the hardenability of the samples. With the addition of 1%Cu, the amount of martensite was increased from 0% to nearly 60% by volume even after a slow cooling rate of 0.5^{o}C/sec. A cooling rate of 3^{o}C/sec caused

formation of 90% martensite phase. The samples containing 2% Cu yielded fully martensitic structures after cooling at a rate of 3^{o}C/sec.

4- For 1% Cu and 2% Cu specimens, the pearlite - martensite two phase mixtures contain some amount of lower bainite as well.

5- In sintered specimens, copper spreads around the particle boundaries. The higher percentage of copper at the particle boundaries seems to enhance the hardenability and cause formation of martensite around the particle boundaries.

REFERENCES

[1] Narasimhan, K.S., *Sintering of Powder Mixtures and the Growth of Ferrous Powder Metallurgy.* Materials Chemistry and Physics, 2001. **67**: p. 56-65.

[2] Singh, R., *Introduction to Basic Manufacturing Process and Workshop Technology,* 2006, New Age International.

[3] Rutz H.G., Graham A.H.., Davala A. B.. *Sinter-Hardening P/M Steels*. in *PM²TEC '97 International Conference on Powder Metallurgy & Particulate Materials*. 1997. Chicago, USA.

[4] German, R.M., *Powder Metallurgy Science*. 2nd Edition ed. 1994, New Jersey, U.S.A,: Metal Powder Industries Federation.

[5] Upadhyaya, G.S., *Powder Metallurgy Technology*, 1997, Cambridge Int Science Publishing.

[6] Vara Prasada Rao, K., *Manufacturing Science & Technology: Manufacturing Processes and Machine Tools*, 2nd ed. 2002, New Age International.

[7] Marucci, M.L., Fillari, G., King, P., Narasimhan, K.S., *A Review of Current Sinter Hardening Technology*, in *PM2004 World Congress*, Vienna, Austria, 2004.

[8] James, W.B. *What is Sinter-Hardening?* in *International Conference on Powder Metallurgy & Particulate Materials*. 1998. Las Vegas, Nevada USA.

[9] Murphy T. F., Baran M.C. *An Investigation into the Effect of Copper and Graphite Additions to Sinter-Hardening Steels*. in *PM² TEC 2004 International Conference on Powder Metallurgy & Particulate Materials*. 2004.

[10] German, R.M., *Sintering Theory and Practice*, 1st ed. 1996, Wiley-Interscience.

[11] Kang, S.L., *Sintering: Densification, Grain Growth and Microstructure*, 2004, Butterworth-Heinemann.

[12] Stuijts, A.L., *Synthesis of Materials From Powders by Sintering* in *Annual Review of Materials Science*, 1973, 3: p. 363-395.

[13] German, R.M., *Liquid Phase Sintering*, 1985, Springer Science & Business Media.

[14] Orban, R.L., *New Research Directions in Powder Metallurgy*, in *Romanian Reports in Physics*, 2004, 56 (3): p. 505-516.

[15] Hatami, S., Malakizadi, A., Nyborg, L., Wallin, D., *Critical Aspects of Sinter-Hardening of Prealloyed Cr-Mo Steel*, in *Material Processing Technology*, 2010, 210 (9): p. 1180-1189.

[16] Engström U., McLelland J., Maroli B., *Effect of Sinter Hardening on the Properties of High Temperature Sintered PM Materials* in *PM²TEC 2002 International Conference on Powder Metallurgy & Particulate Materials*., 2002.

[17] *Höganäs Handbook for Sintered Components: Sintered Iron Based Materials*, in *PM School Handbook*, 2013.

[18] Chagnon, F., Trudel, Y., Effect of Sintering Parameters on Mechanical Properties of Sinter Hardened Materials, in Advances in Powder Metallurgy & Particulate Materials, 1997, 3 (14).

[19] Nyberg, I., Schmidt, M., Thorne, P., Gabler, J., Feldbauer, S., Jesberger, T.J., Effect of Sintering Time and Cooling Rate on Sinter Hardenable Materials, International Conference on Powder Metallurgy & Particulate Materials, 2013, Las Vegas, NV.

[20] Engstöm, U., *Evaluation of Sinter Hardening of Different PM Materials*. in *PM² TEC 2000 International Conference on Powder Metallurgy & Particulate Materials*. 2000. New York.

[21] James, B., *Recent Developments in Ferrous Powder Metallurgy Alloys.* Powder Metallurgy, 1994.

[22] McLelland,J. Mars O., Jesberger T. J.,. *Sintering Furnace Cycle Influence on Sinter Hardened Part Parameters*. in *PM² TEC 2001 International Conference on Powder Metallurgy & Particulate Materials*. 2001.

[23] Chagnon F., T.Y. *Effect of Copper Additions on Properties of 1.5% Mo Sintered Steels*, in *PM² TEC 2002 International Conference on Powder Metallurgy & Particulate Materials.* . 2002. Orlando.

[24] Lindsley B., Rutz H., *Effect of Molybdenum Content in PM Steels*, Advances in Powder Metallurgy & Particulate Materials, 2008.

[25] Sokolowski, P.K., Lindsley, B., Hanejko, F.G., *Introduction of a New Sinter Hardening PM Steel*, in *2008 World Congress on Powder Metallurgy & Particulate Materials*, 2008, Washington, D.C.

[26] Simkulet V., Selecka M., *Effect of Manganase on Fracture of Premix and Hybrid Fe-0.85Mo-XMn-0.3C Sintered Steel.* Powder Metallurgy Progress, 2006. 6 (4): p. 156-163.

[27] Wong-Ángel, W.D., Téllez-Jurado, L., Chávez-Alcalá, J.F., Chavira-Martínez, E., Verduzco-Cedeño, V.F., *Effect of Copper on the Mechanical Properties of Alloys Formed By Powder Metallurgy*, in *Materials & Design*, 2014, 58: p. 12-18.

[28] Chagnon, F., Gagne, M., *Effect of Graphite and Copper Concentrations And Post Sintering Cooling Rate on Properties of Sinter Hardened Materials*, in *2000 International Conference on Powder Metallurgy & Particulate Materials*, 2000, New York, N.Y.

[29] Bocchini G. F., Rivolta B., Silva G., Poggio E., Pinasco M. R.,. Ienco M.G, *Microstructural and Mechanical Characterisation of Some Sinter Hardening Alloys and Comparisons with Heat Treated PM Steels.* Powder Metallurgy, 2004. **47**(4): p. 343-351.

[30] Mazancova, E., Jonsta, Z., Wyslych, P., Mazanec, K., *Acicular Ferrite and Bainite Microstructure and Properties and Comparison of Their Physical Metallurgy Response*, in *14. International Metallurgy & Material Conference*, 2005. 5: p. 24-26.

[31] Bhadeshia H.K.D. H., *Bainite in Steels Transformations, Microstructure and Properties*. 2nd Edition ed. 2001, Cambridge.

[32] Ridal K.A. and McCann J., Physical Properties of Martensite and bainite , special report, 93, Iron and Steel Institute (London) (1965) 147-148

[33] Feng Chun , Fang Hong-sheng, Zheng Yan-kang , Bai Bing-zhe, Mn-Series Low-Carbon Air-Cooled Bainitic Steel Containing Niobium of 0.02%. Journal of Iron And Steel Research, Internatıonal. 2010, 17(4): 53-58.

[34] Habraken L. Bainitic Transformation of Steels [J]. Revue de Metallurgie , 1956, 53(2): 930.

[35] Fang Hong-sheng , Bai Bing-zhe. Zheng Xiu-hua. Morphology and Phase Transformation of Granular Bainite and Granular Structure [J]. Acta Metallurgica Sinica , 1986. 22 (4): 283

[36] Neilan, A., Ropar, S., Hu, B., Warzel, R., *Characterization of Nickel Additions to Heat Treated Iron - Copper - Carbon Materials*, in *PM2014 World Congress on Powder Metallurgy and Particulate Materials*, 2014, Orlando.

[37] Kılıç, G., *Sinter Hardening Studies of Distaloy DH Powders With Varying Carbon Contents*, 2013, M.S. Thesis, Middle East Technical University, Ankara, Turkey.

[38] Öge, M. A., *Demir Esaslı Astaloy Mo ve Distaloy DH Alaşımlarında Sinterleme ile Sertleştirme*, M.S. Thesis, 2013, TOBB University of Economics and Technology, Ankara, Turkey.